Effects of Steam-Induced Diagenesis on Heavy-Oil Production in Miocene-Pleistocene Sands from Kern River Oil Field, California*

Robert A. Horton, Jr.[1], Larry Knauer[3], Dawne Pennell[2], and Kay Coodey[1]

Search and Discovery Article #20076 (2009)
Posted September 30, 2009

*Adapted from oral presentation at AAPG Annual Convention, Denver, Colorado, June 7-10, 2009

[1]Grants, Research, and Sponsored Programs, California State University at Bakersfield, Bakersfield, CA (rhorton@csub.edu; s_pomai@yahoo.com)
[2]Aera Energgy LLC, Bakersfield, CA (dapennell@aeraenergy.com)
[3]Chevron U.S.A. Inc, Bakersfield, CA (larryknauer@chevron.com)

Abstract

Kern River oil field in Kern County, California was discovered in 1899. Although over two-billion barrels of oil have been produced from this field, substantial reserves remain. The reservoir consists of braided alluvial sands and gravels of the Kern River Formation (Miocene-Pleistocene). Currently heavy oil (12° - 13° API) is produced using steam injection. Steam injection typically results in good production from well sorted medium to very coarse sands, but less well sorted sands and gravels are commonly bypassed and remain unproduced, with residual oil saturations 10-30 saturation units higher than the adjacent rock despite heating to temperatures of 220° F and greater. This study examined mineralogy and pore geometry in sands that had not been heated, sands that had been heated but were not drained, and sands that had been swept of hydrocarbons by steam. The sands of the Kern River Formation are composed predominantly of quartz, K-feldspars (orthoclase and microcline), plagioclase (andesine-oligoclase), microphanerites of granitic composition, and minor biotite (1-3%), reflecting their source from granites in the southern Sierra Nevada. Clays of detrital and authigenic origin typically make up 5-13% of the rocks. The clays are dominated by mixed illite/smectite with 80-90% smectite layers; there is also minor kaolinite. Samples that have been heated but not drained of oil are generally similar to unheated samples. Introduction of steam into the rocks as the sands were drained of oil resulted in the breaking apart of microphanerites, dissolution of feldspars, and a slight increase in the amount of clays; notably there is no significant change in total porosity. Texturally there are significant differences in the distribution of clays and the geometry of the pore networks between unsteamed sands and those that have been swept of hydrocarbons. The disintegration of microphanerites and subsequent rotation of the grain fragments has changed the sorting and reduced pore-throat diameters. Recrystallization and precipitation of mixed illite/smectite has resulted in an increase in the amount of pore-filling clay cements, including as bridges across pore throats that may have restricted fluid flow. The extent to which this may have affected subsequent production is under investigation.

References

Dickinson, W.R., 1970, Interpreting detrital modes of graywacke and arkose: Journal of Sedimentary Petrology, v. 40, p. 695-707.

Dott, R.H., 1964, Wacke, graywacke, and matrix — what approach to immature sandstone classification?: Journal of Sedimentary Petrology, v. 34, p. 625-632.

Kodl, E.J., 1988, Texaco, unpublished in-house report.

How does steam injection affect reservoir sands and how does this affect subsequent production?

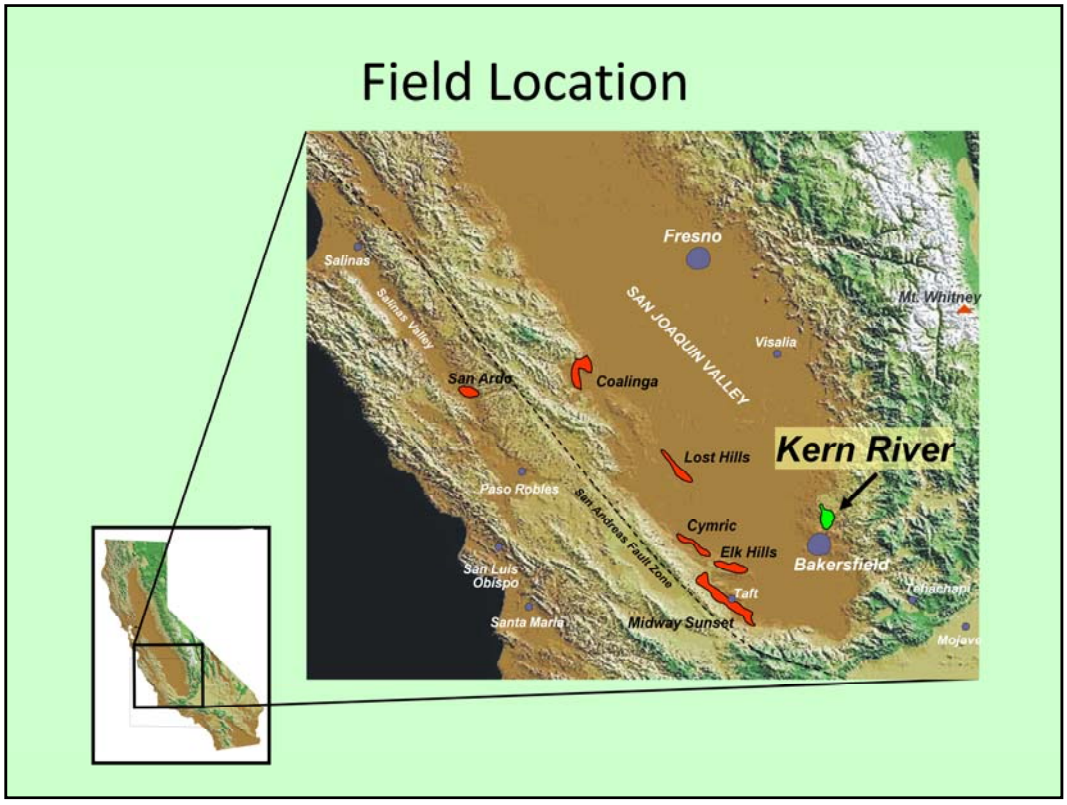

Kern River is the largest oil field on the east side of the San Joaquin basin. Production recently passed the 2-billion barrel mark. The field is located within the Kern River alluvial fan complex at the mouth of the Kern River north of Bakersfield.

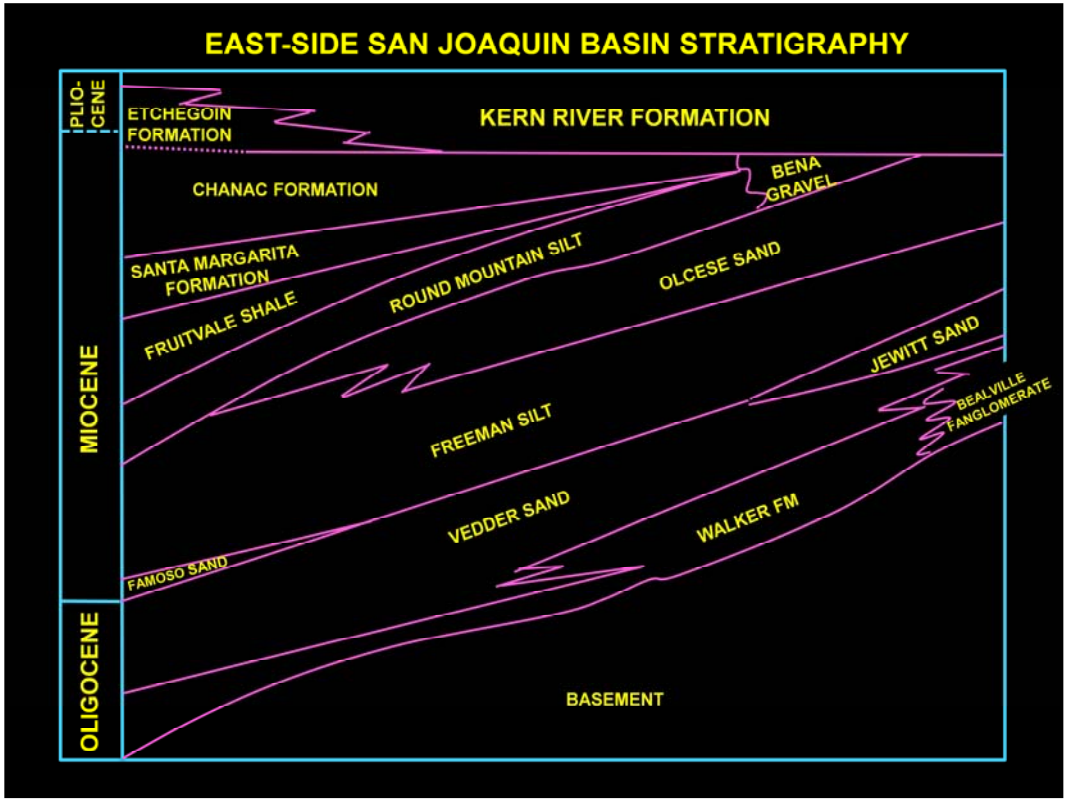

This is a simplified version of the regional stratigraphy. Oil at Kern River is produced from the Kern River Formation, a non-marine sequence of silts, sands, and gravels. The Kern River Formation lies atop a series of alluvial and shallow-marine sands, silts, and gravels derived from erosion of the Sierra Nevada during the Cenozoic. Historically the Kern River Formation has been assigned to the Pliocene but recent data indicate that the lower portion of the Kern River Formation is Miocene in age.

Kern River Oil Field Geologic Framework: Structure

- Gentle dipping homocline (3.5 degree to the SW)

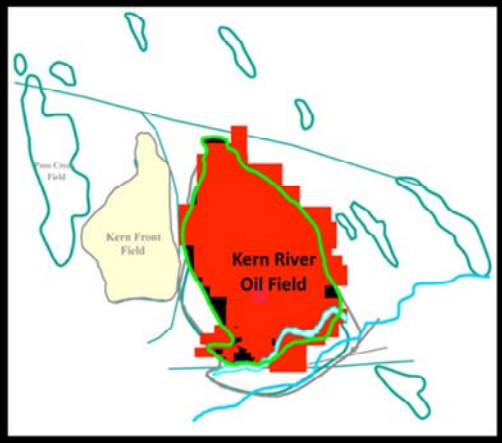

The structure is relatively simple with homoclinal beds dipping gently to the southwest. The field is bounded on the north, west, and south by normal faults with offsets of more than 100 ft. There are also several smaller faults within the field.

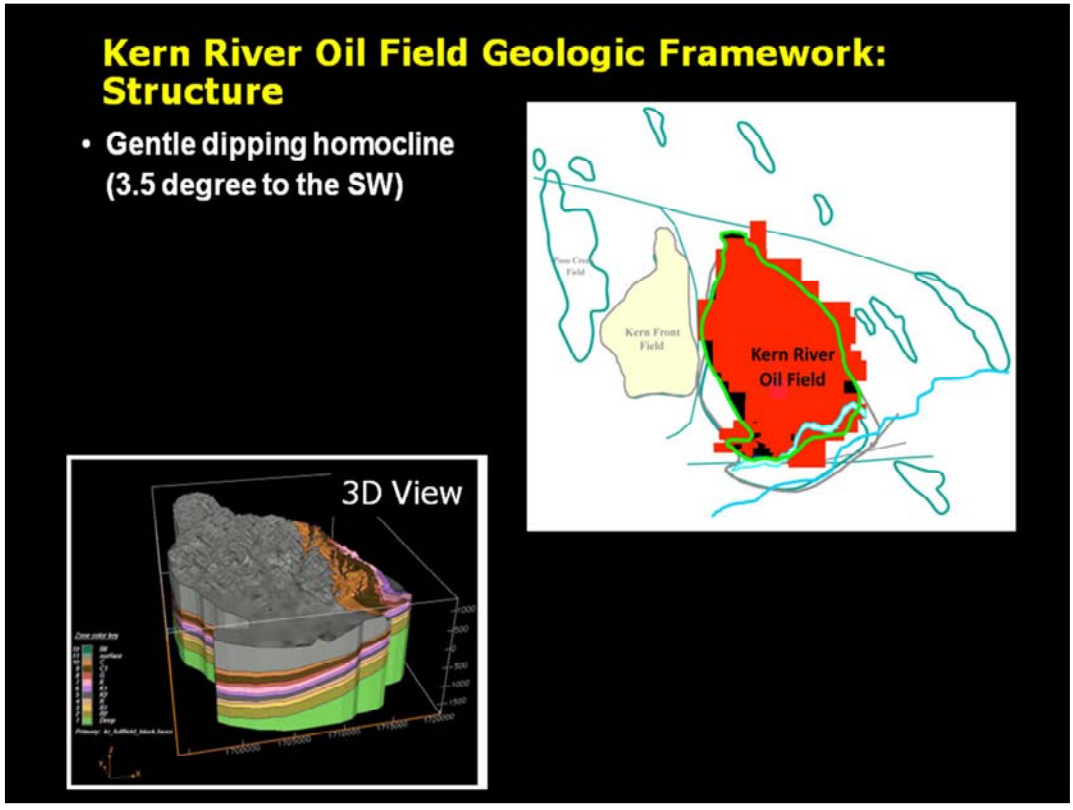

The structure is relatively simple with homoclinal beds dipping gently to the southwest. The field is bounded on the north, west, and south by normal faults with offsets of more than 100 ft. There are also several smaller faults within the field.

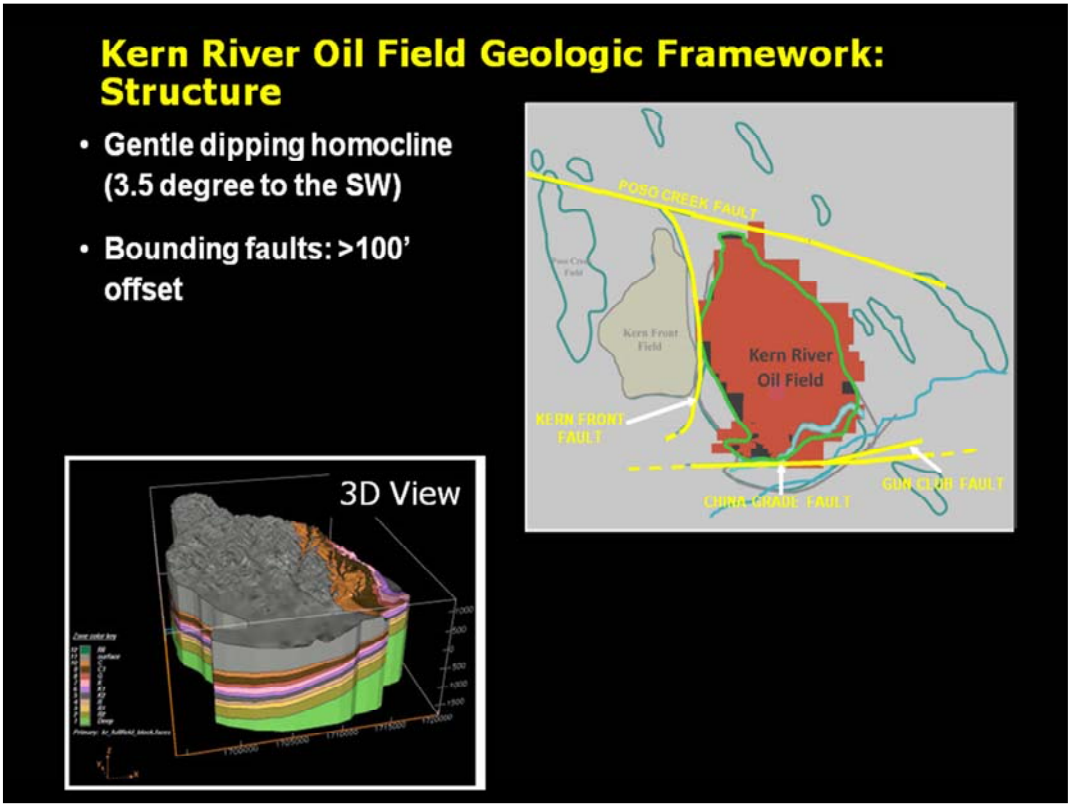

The structure is relatively simple with homoclinal beds dipping gently to the southwest. The field is bounded on the north, west, and south by normal faults with offsets of more than 100 ft. There are also several smaller faults within the field.

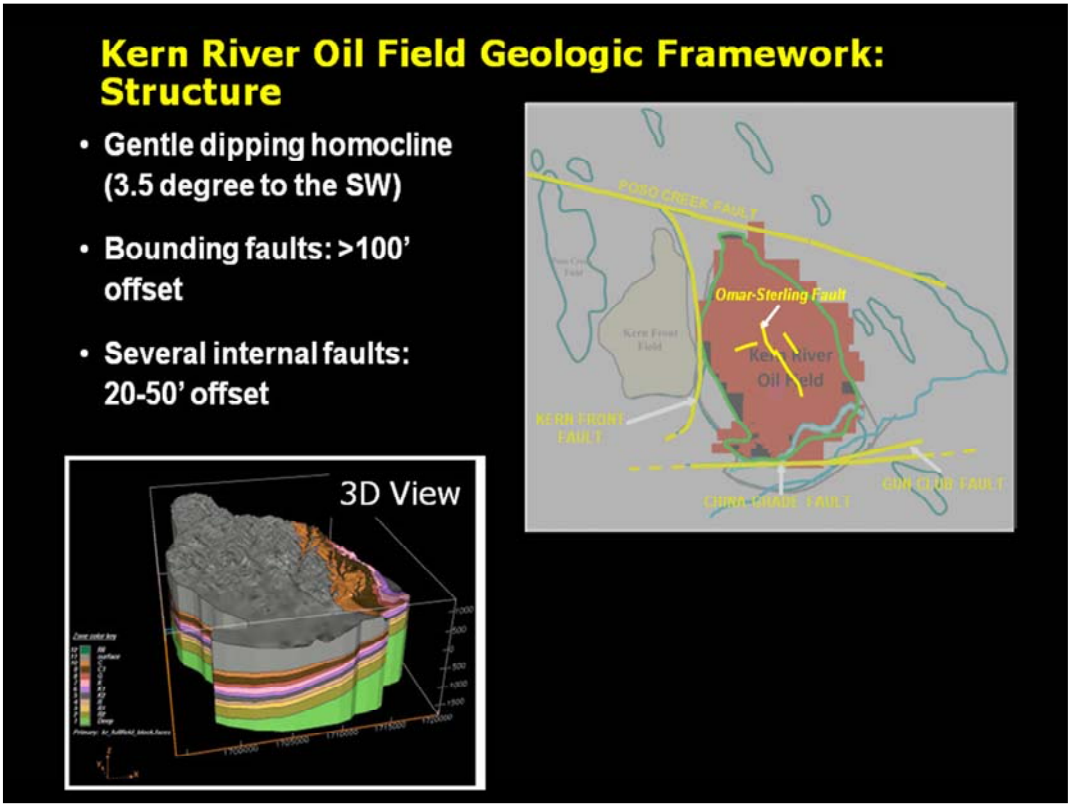

The structure is relatively simple with homoclinal beds dipping gently to the southwest. The field is bounded on the north, west, and south by normal faults with offsets of more than 100 ft. There are also several smaller faults within the field.

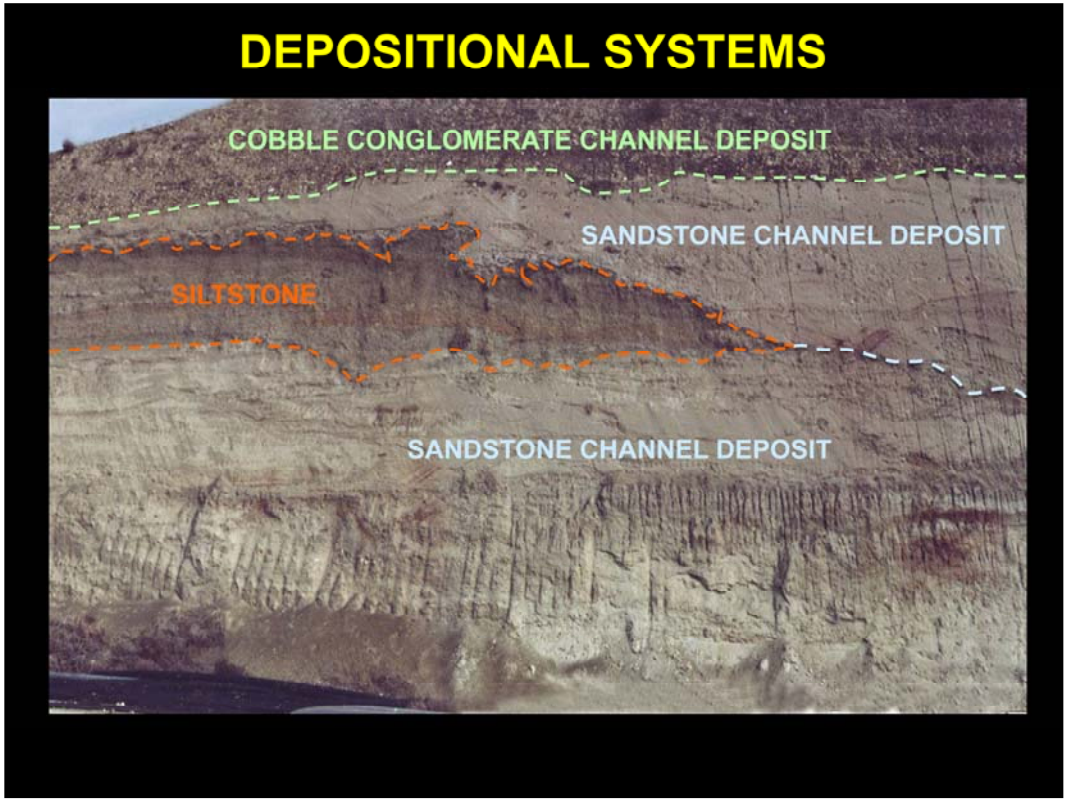

The sediments consist of sandstones and conglomerates deposited in channels and more widespread laminated siltstones deposited as overbank or flood-plain deposits.

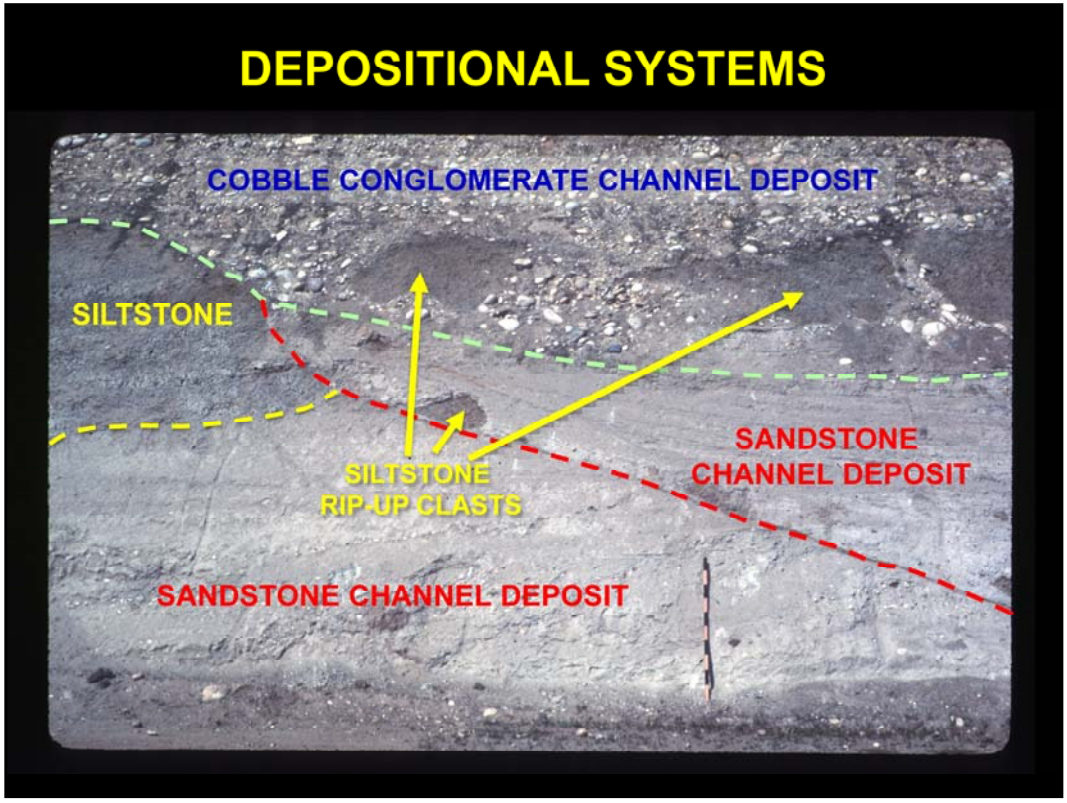

Here is another view showing the relationships between channel deposits and siltstone. Notably the conglomerates and sandstones commonly contain rip-up clasts derived from the siltstones.

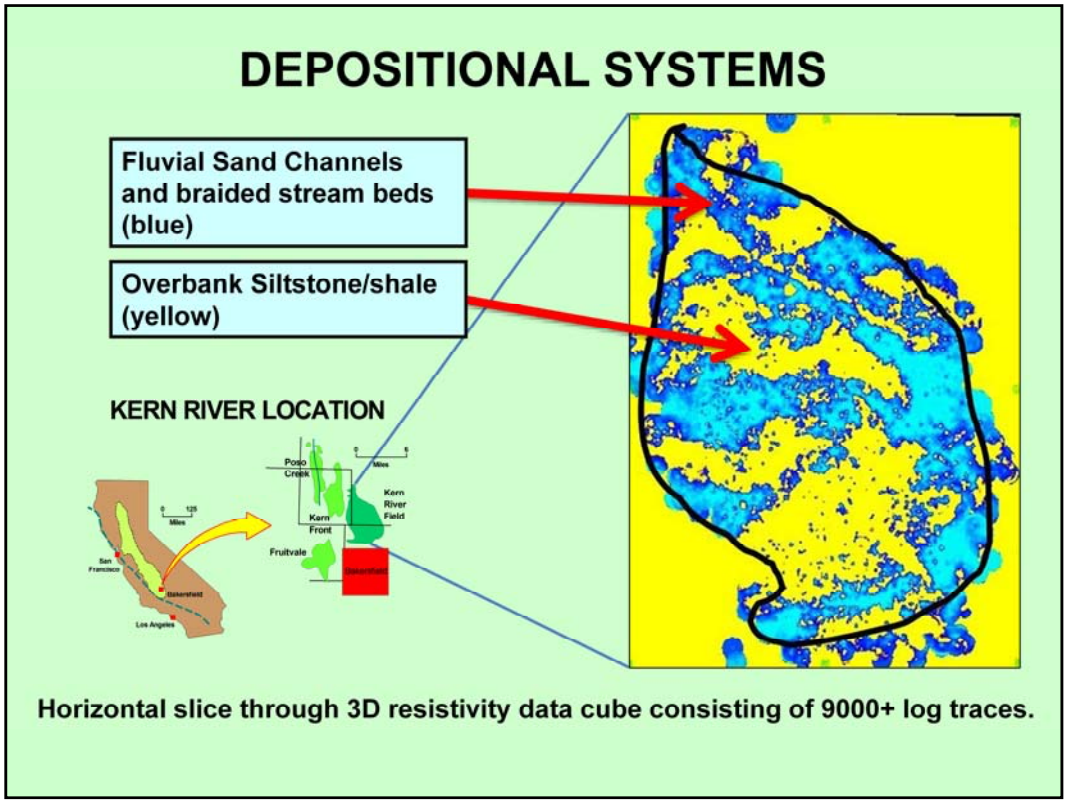

This is a horizontal resistivity slice based on more than 9000 well logs. The distribution of sandstone and conglomerate channels is shown in blue and the more widespread siltstones are shown in yellow.

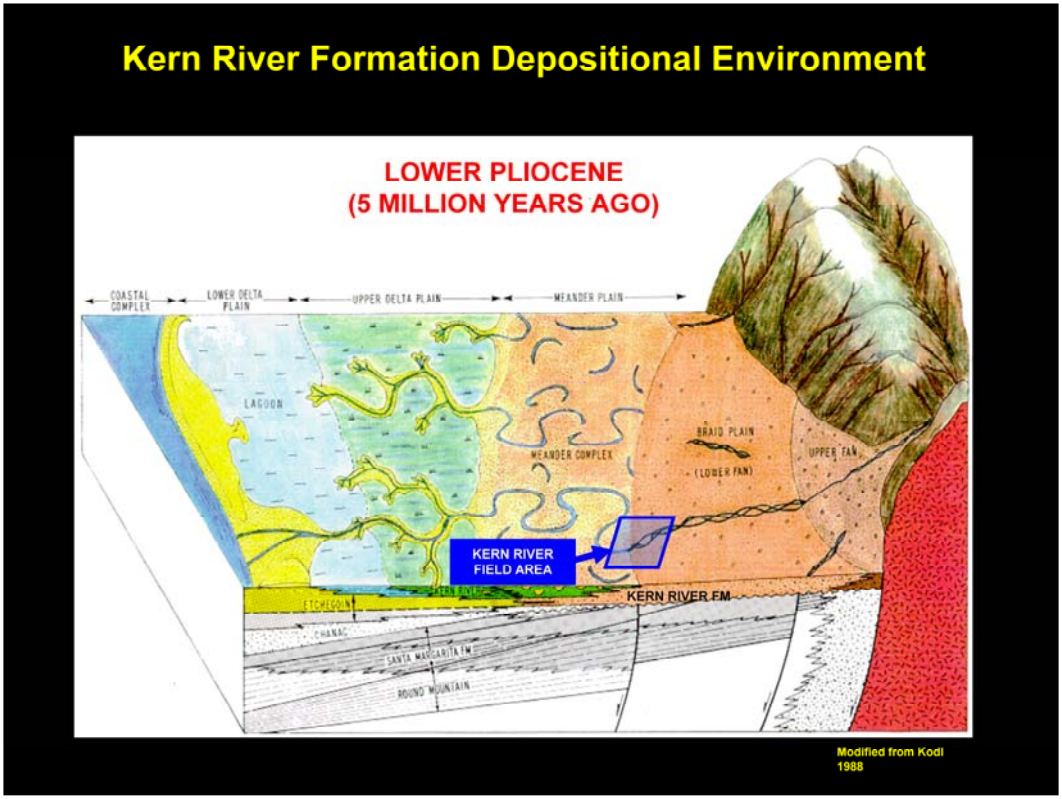

Surprisingly there have not been any published detailed studies of the Kern River Formation depositional system in this area that made use of the abundant outcrops and core samples that are available. This diagram is adapted from Kodl (1988) and we interpret the Kern River sediments as having been deposited in the transition between the strictly braided stream complex and the meandering stream regime, but this is an area that is ripe for further study.

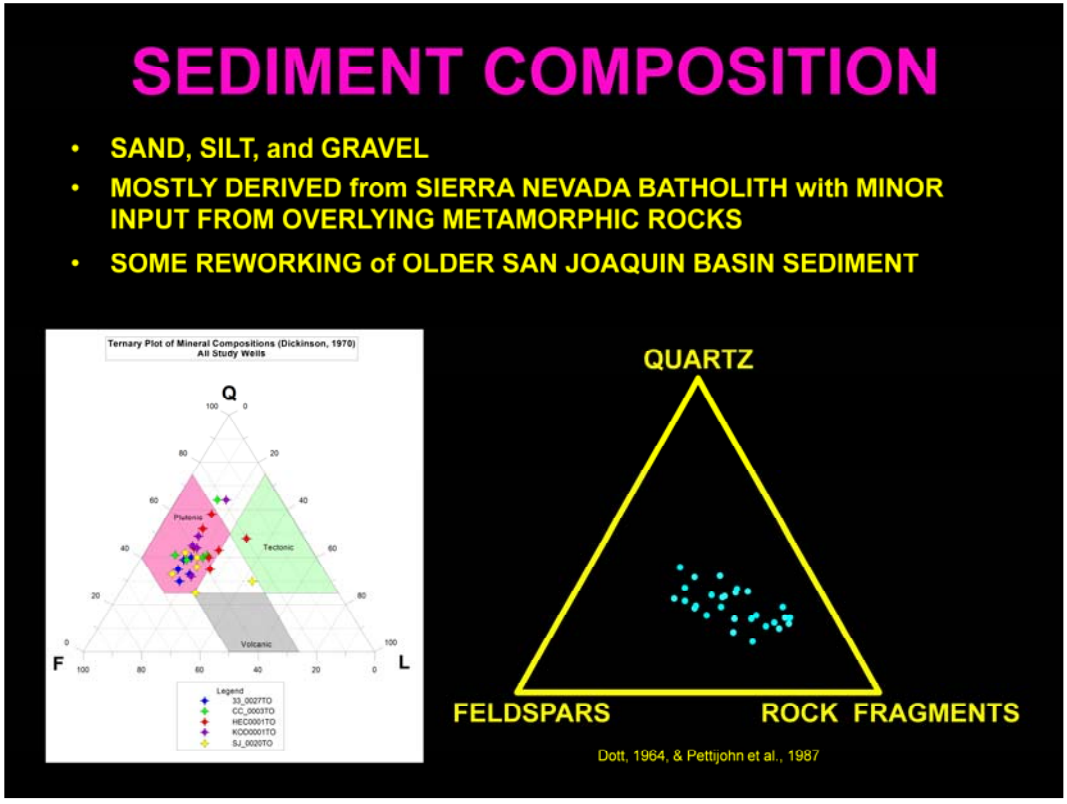

The sediments are mainly sand, silt, and conglomerate; there is very little shale. They are mostly derived from the Sierra Nevada batholith with minor input from the overlying metamorphic rocks. The first ternary diagram shows sandstone point-count data for sandstones plotted according to the scheme of Dickinson (1970). The data fall clearly in the plutonic field. The second ternary diagram shows sandstone point-count data plotted according to the scheme of Dott (1964) and Pettijohn et al. (1987); the sands contain a large percentage of microphaneritic rock fragments. The utility of this type of plot will be shown shortly.

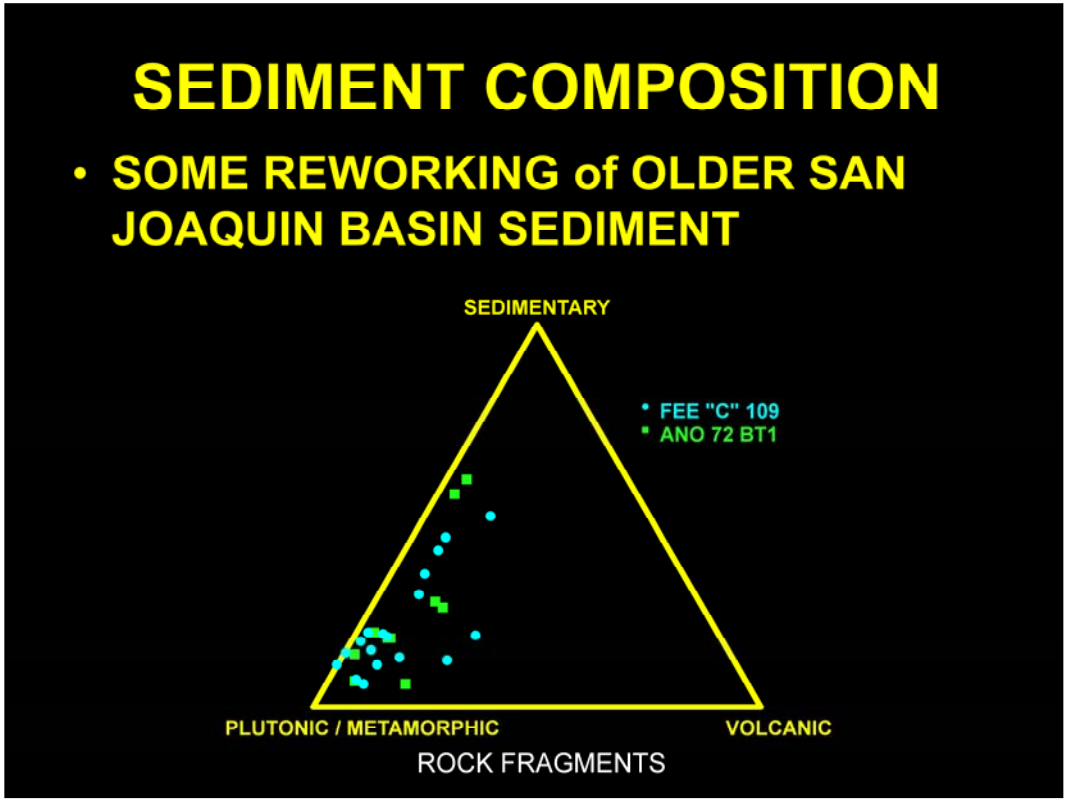

Rock Fragments are dominated by granitic microphanerites but there are also sedimentary rock fragments derived from older San Joaquin basin sediments.

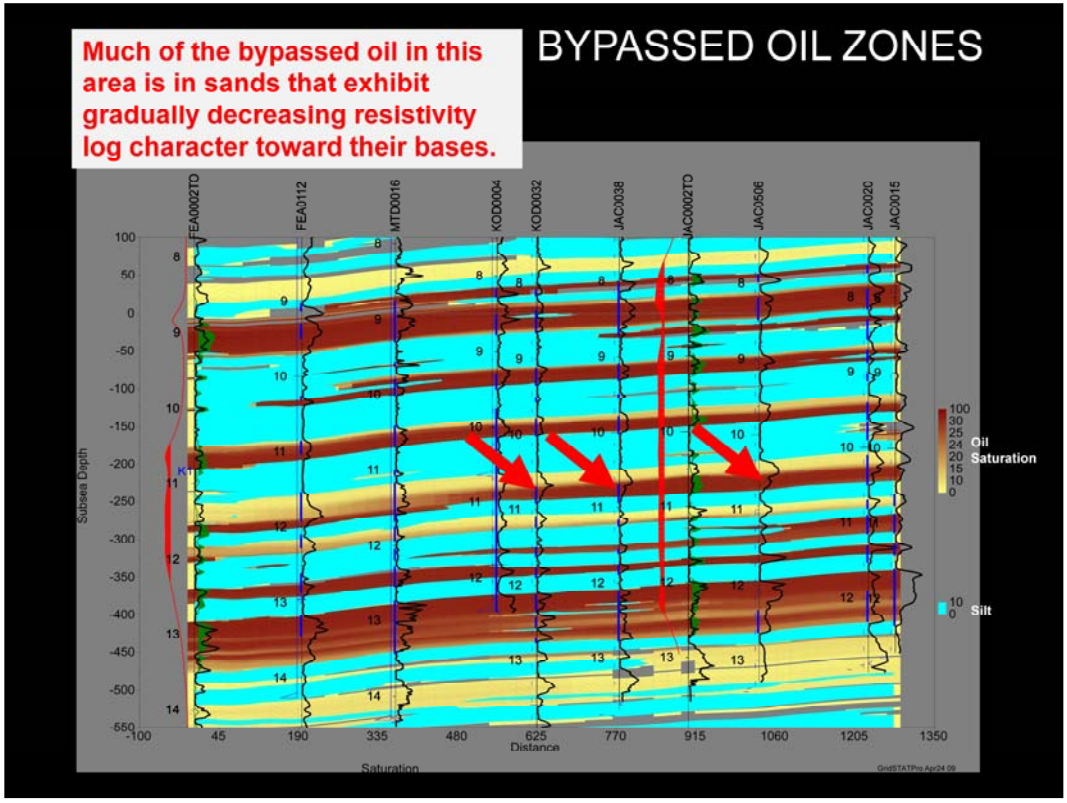

Here is a cross section showing residual oil saturation following steam-enhanced production. Siltstones with low permeability are shown in blue. Potential reservoir rocks are shown in yellows and browns, with yellow indicating that oil has been removed and brown showing zones of bypassed oil. There are two temperature logs showing the heated zones. Much of the bypassed oil resides in sands exhibiting gradually decreasing resistivity log signatures at their bases. Typically the higher resistivity intervals are interpreted as sands and the lower resistivity intervals as silts. However, if these gradually decreasing resistivity signatures are simply due to a gradual reduction in grain size from sand to silt, the sharp boundary between produced and bypassed zones is hard to explain.

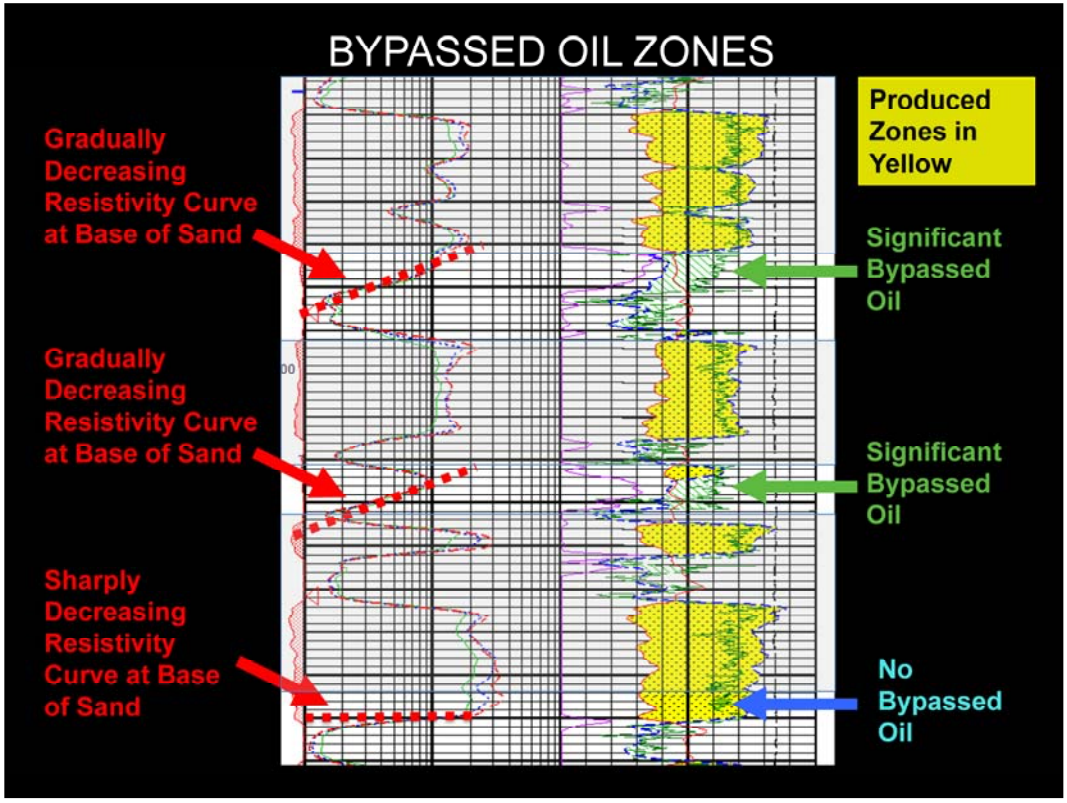

Here is a log with resistivity on the left and oil saturation on the right. Produced sands are shown in yellow. At the bases of the upper two sands there are significant zones of bypassed oil shown in green. The log signatures for both of these sands exhibit gradually decreasing resistivity values across the bypassed-oil intervals. The lower sand's resistivity profile shows a sharp decrease at its base and there is no bypassed oil.

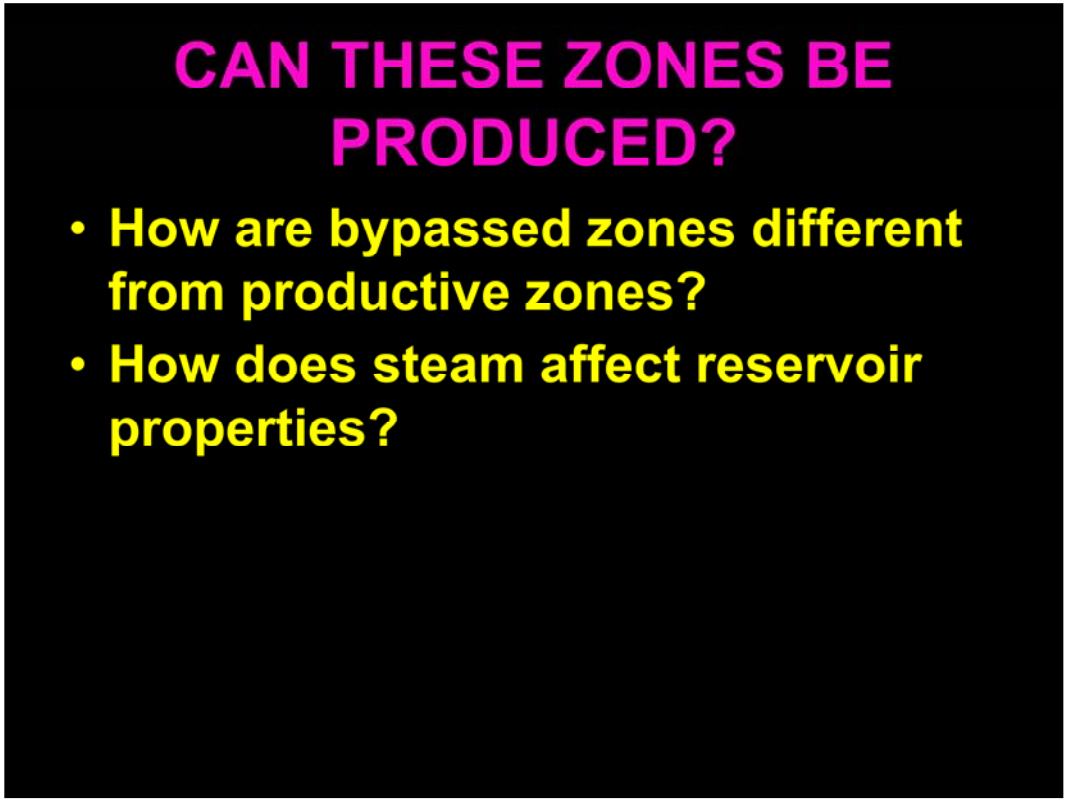

The bypassed zones contain a significant volume of oil. In order to address whether or not these can be produced, it is first necessary to determine the lithologic differences between the bypassed zones and the productive sands. Also, as the bypassed zones already have been heated it is necessary to determine what effects this may have had on reservoir properties.

The first step in answering these questions was to identify and examine cores from bypassed intervals. This example, which is typical of these intervals, shows a rather abrupt change from moderately sorted sand to poorly sorted gravel. Notably the sand at the top of the interval was produced while the gravel was not.

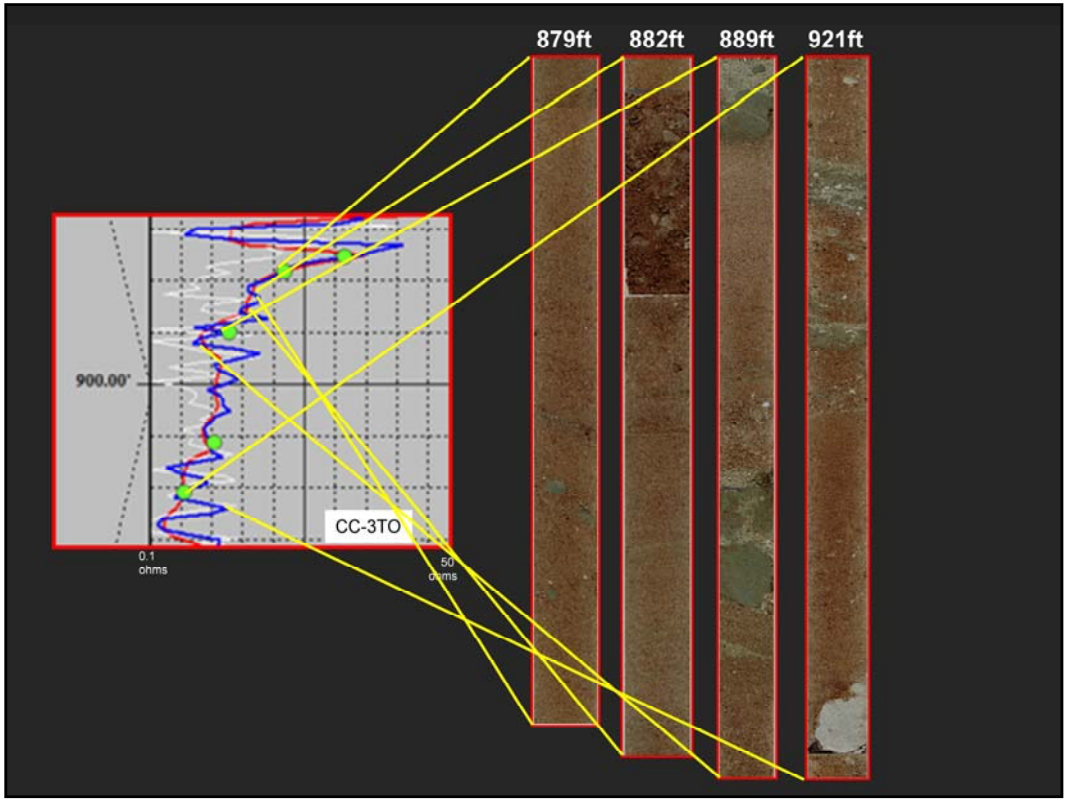

On the left is a typical resistivity log from one of these zones. The cores on the right show the change from moderately sorted sand at the top to poorly sorted gravel toward the base. The green dots show locations of samples collected for analysis.

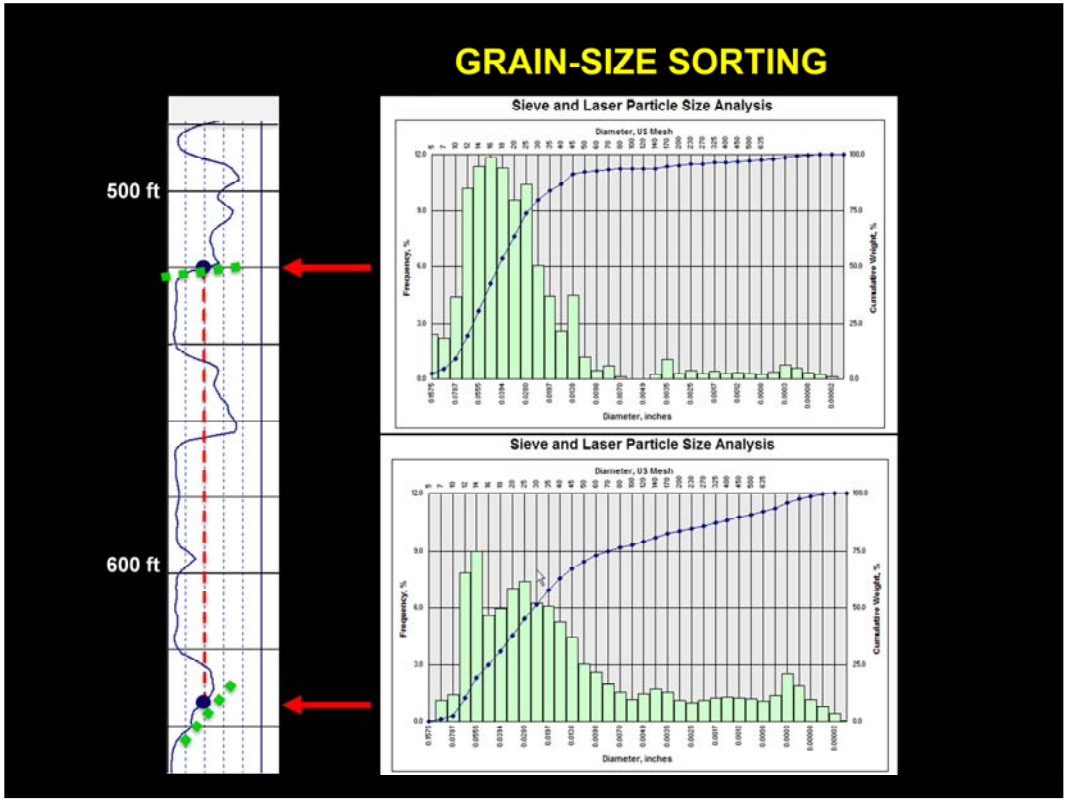

Here are grain-size profiles for samples from the bases of two sands. The upper sand has a sharply decreasing resistivity curve associated with its base and is moderately well sorted sand. The lower sand has a gradually decreasing resistivity curve associated with its base and sediment from this interval is poorly sorted sand with significant amounts of fine material in addition to the sand. Notably, both of these samples were collected from sediments with the same resistivity value, so resistivity is controlled by more than just mean particle size.

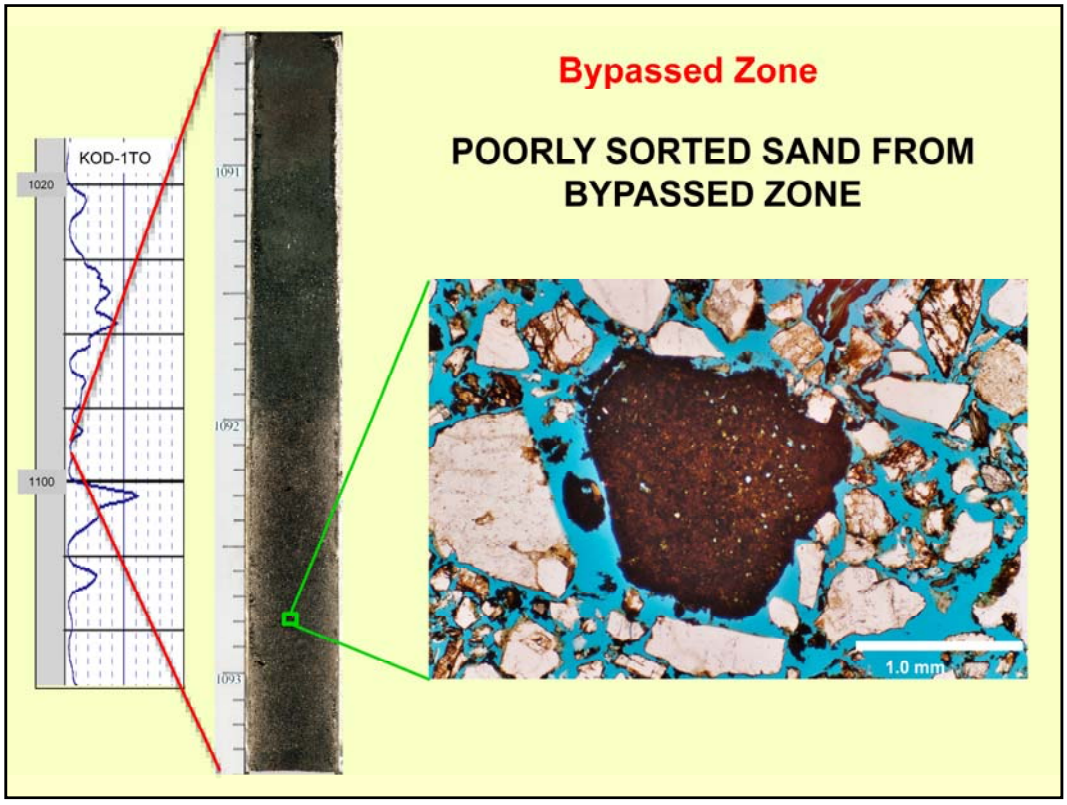

Here is a thin section from one of these bypassed zones illustrating the poorly sorted nature of the sand. Note the large shale clast in the center.

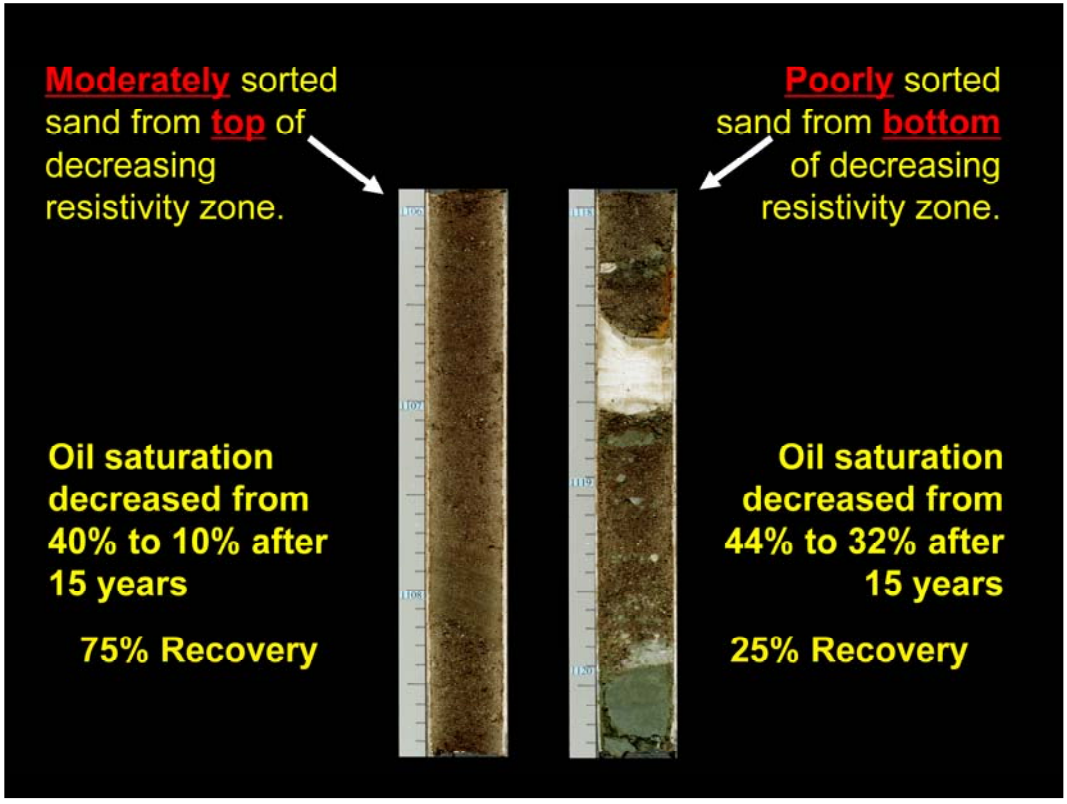

On the left is a moderately sorted sand from the top of a decreasing resistivity zone, and on the right is a poorly sorted gravel from the bottom of the same zone. After 15 years of steam injection, oil saturation at the top of the zone decreased form 40% to 10% for a rather respectable 75% recovery rate. However, over the same time period, oil saturation at the bottom of the zone decreased from 44% to 32% for only a 25% recovery rate.

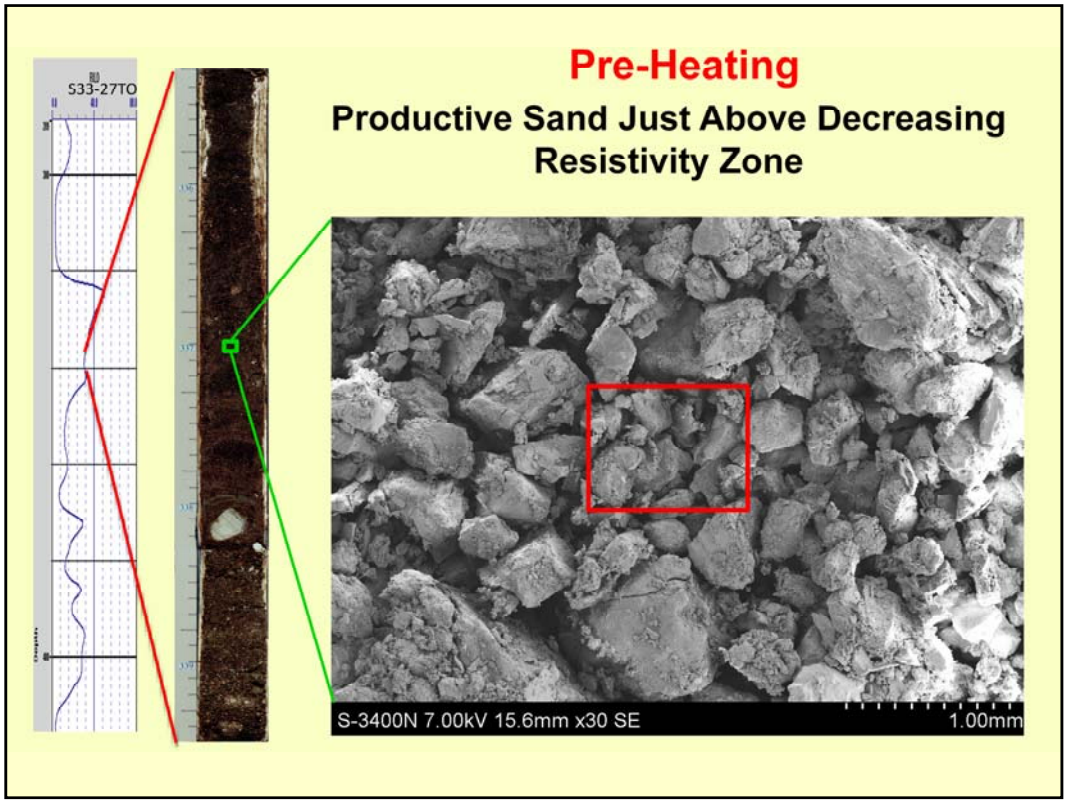

Here is a moderately to well sorted sand from a core taken prior to heating. This sand was ultimately drained of oil. The next slide will zoom in on the enclosed area.

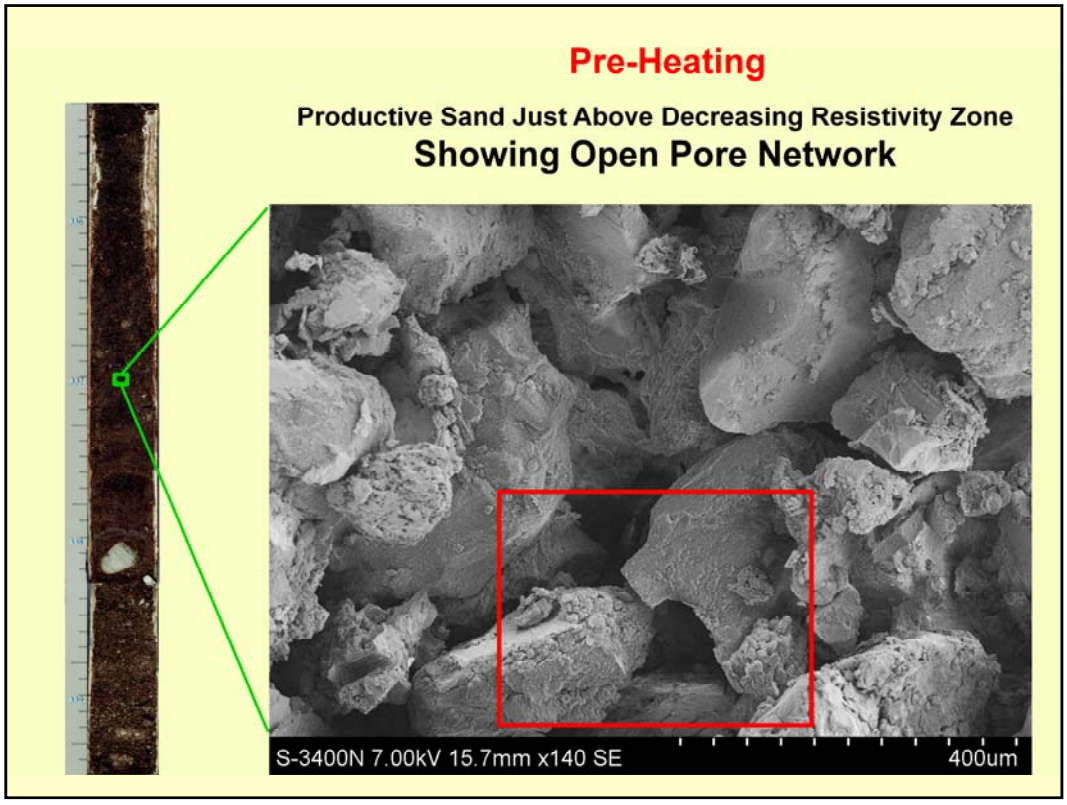

The sand has an open, interconnected pore network. The next slide will zoom in on the enclosed area.

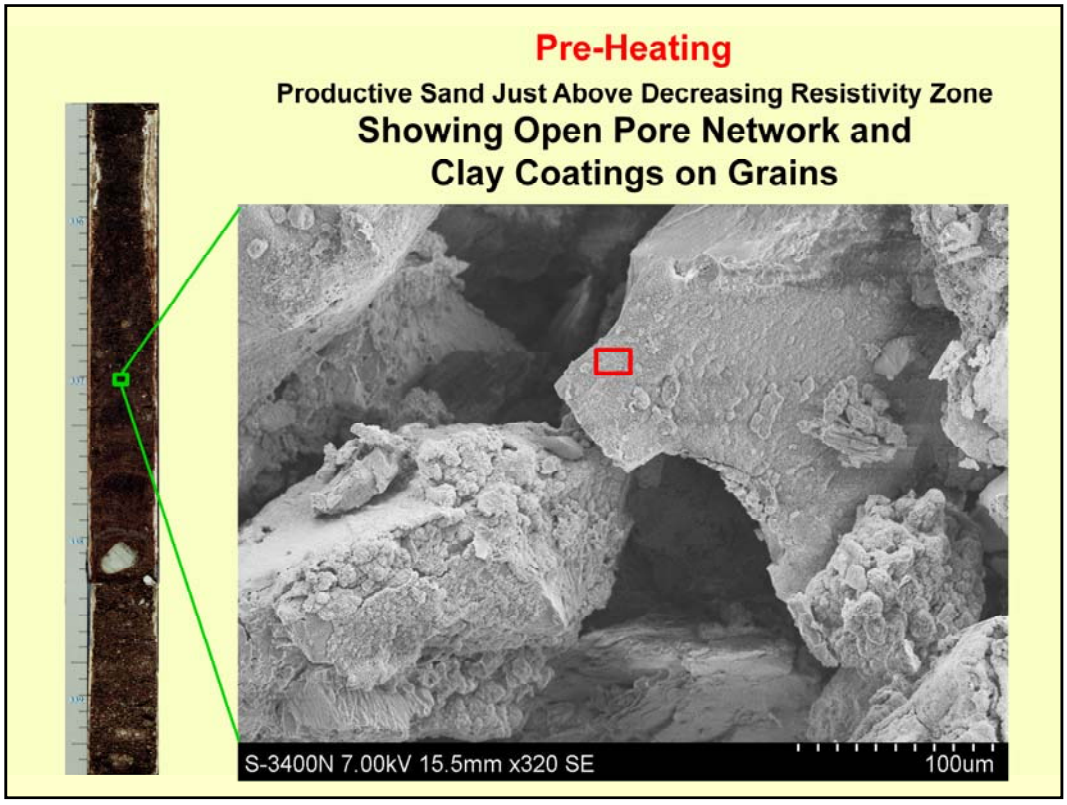

We can look down into these pores and see how clean they are and how well they interconnect. At this scale we can also see that the grains are covered with thin coatings of clay. The next slide will zoom in on the enclosed area.

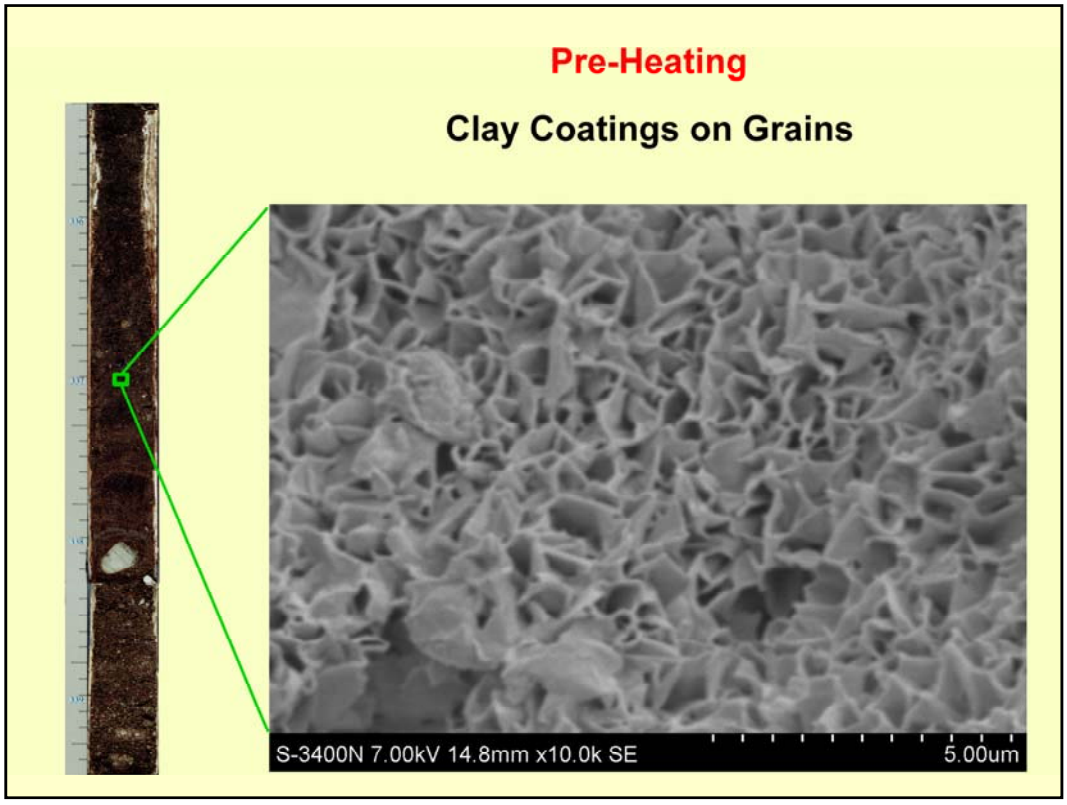

The clay coating consists of a fine meshwork of clay crystals, identified as smectite using x-ray diffraction analysis. The clays exhibit significant intercrystalline pore volume, but note that the pores are roughly ½ micron in diameter.

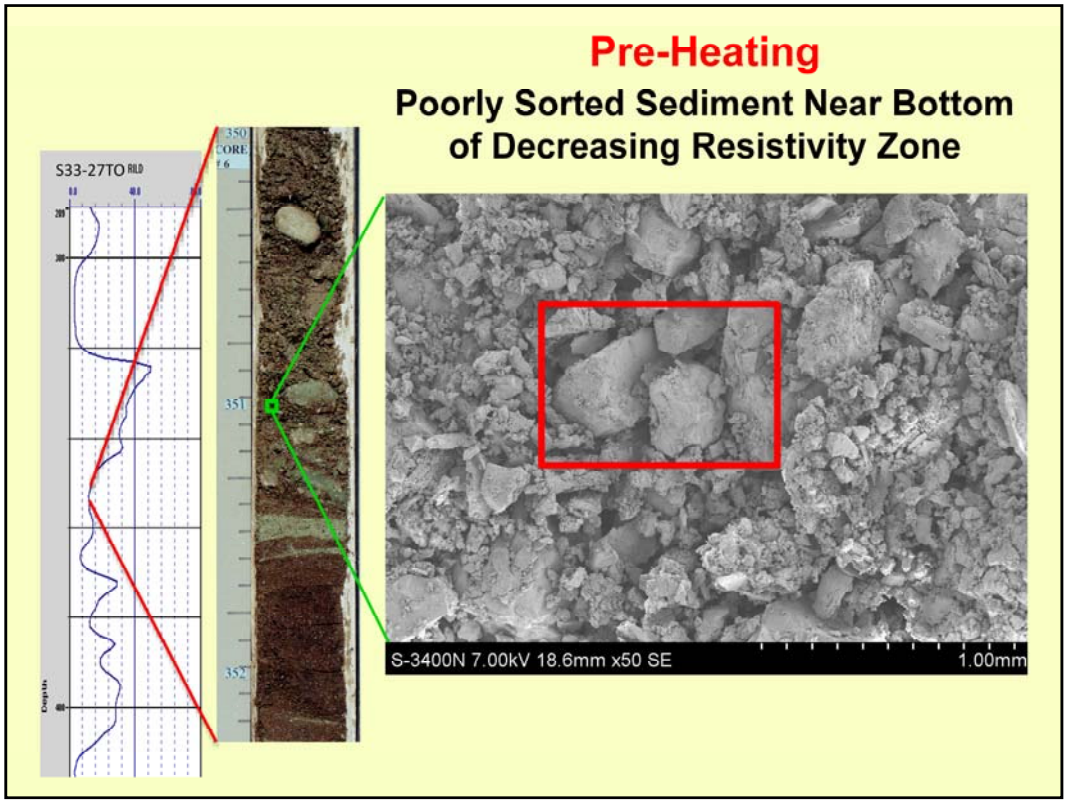

This sample is from lower in the same decreasing-resistivity zone and was taken before heating. The sediment is poorly sorted at both the core scale and at the microscopic scale. The next slide will zoom in on the enclosed area.

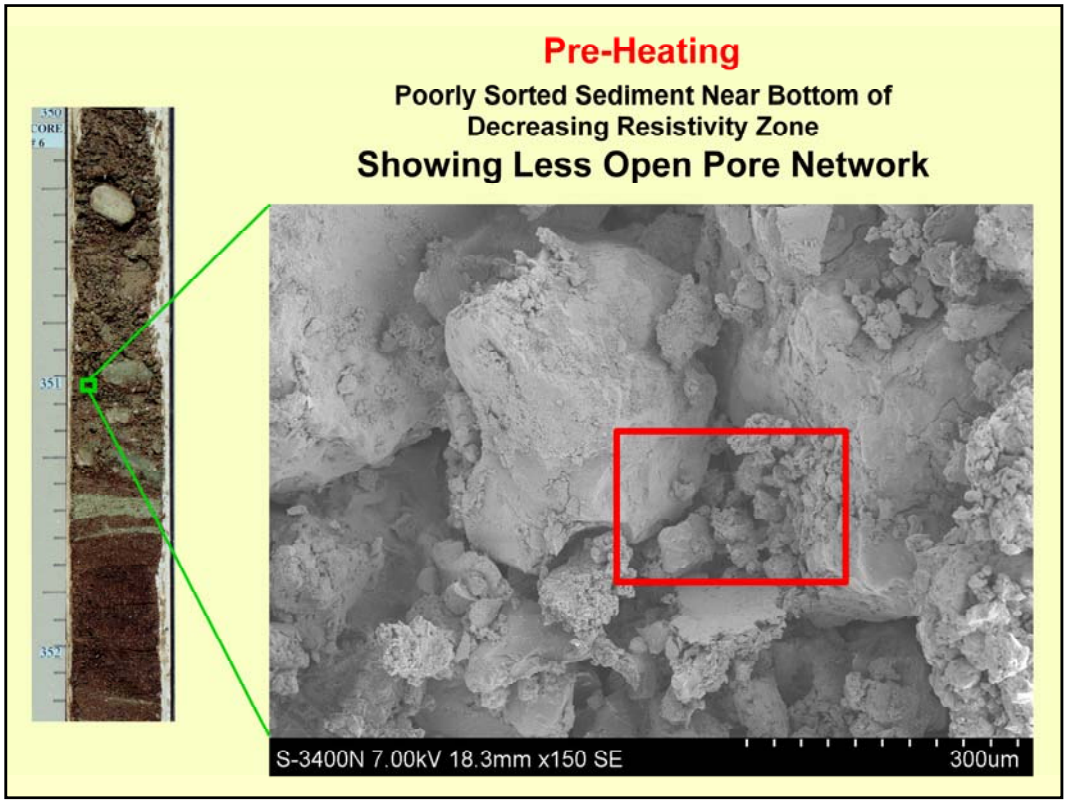

The pore spaces between the sand grains contain grains of finer sediment. Now we'll zoom in again...

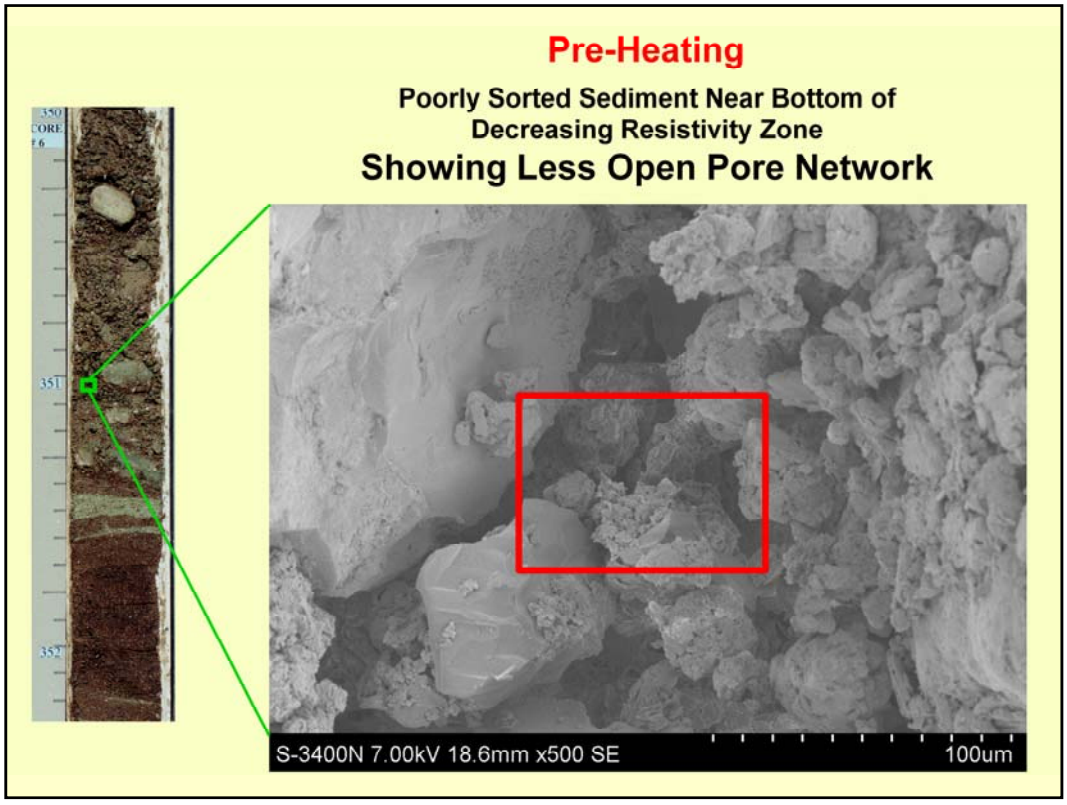

Even smaller grains are visible between the small grains shown in the last slide. The next slide will zoom in on the enclosed area.

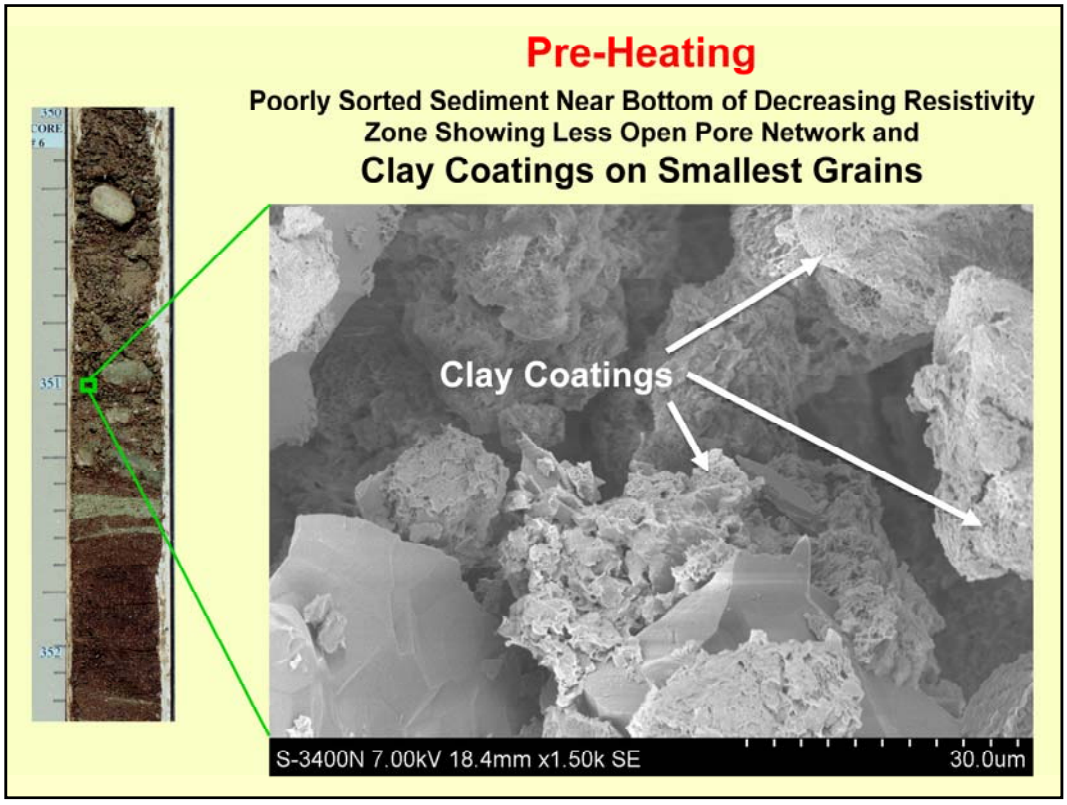

At a magnification of 1500 x still smaller grains are visible in the spaces between the small particles seen in the previous slide. At this scale clay coatings are visible on many of the grains.

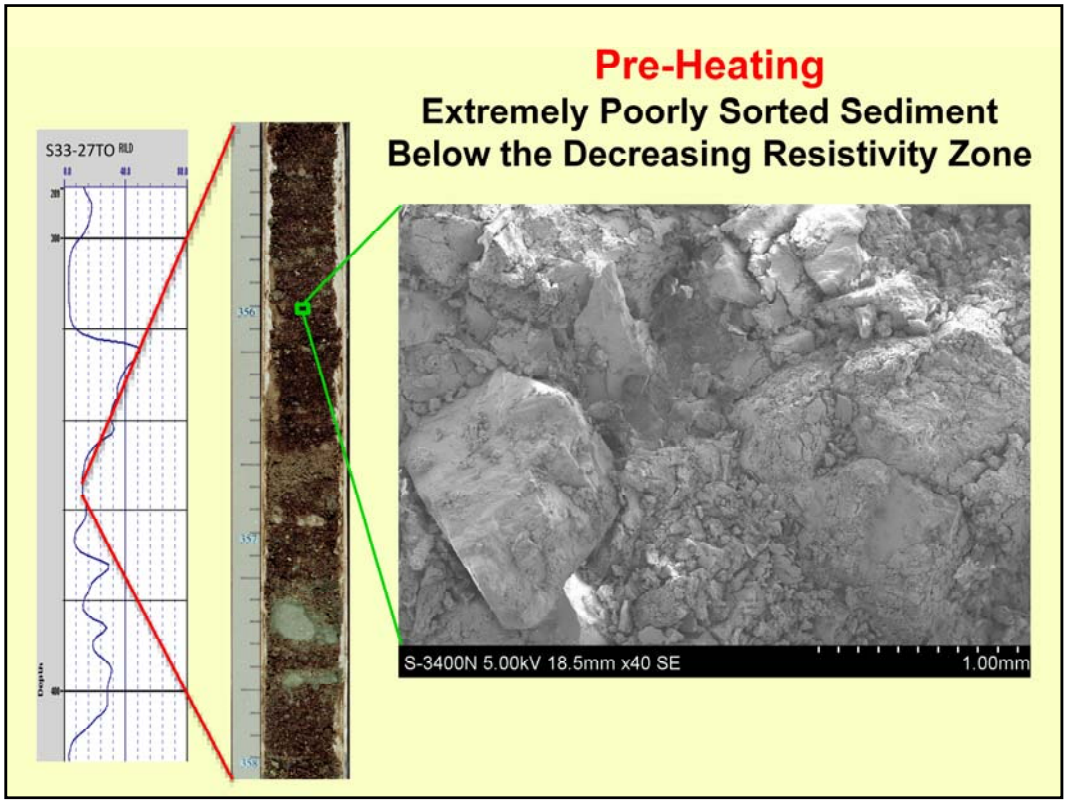

This pre-heating sample is from the base of the low-resistivity zone. Although the core obviously contains oil, there is virtually no porosity visible at the scale of this low-magnification SEM image.

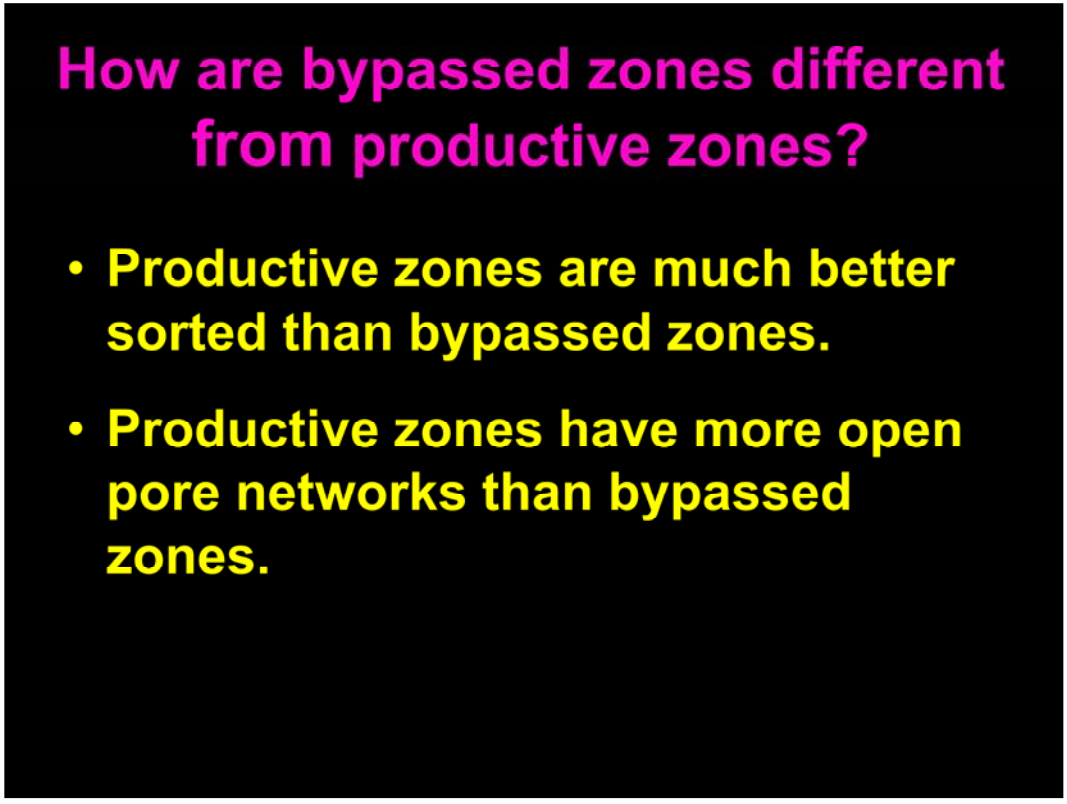

Summarizing, the bypassed zones differ from the productive zones in that the productive zones are composed of moderately to well sorted sand with relatively open pore networks while the bypassed zones are composed of poorly sorted sand and gravel with less open pore networks.

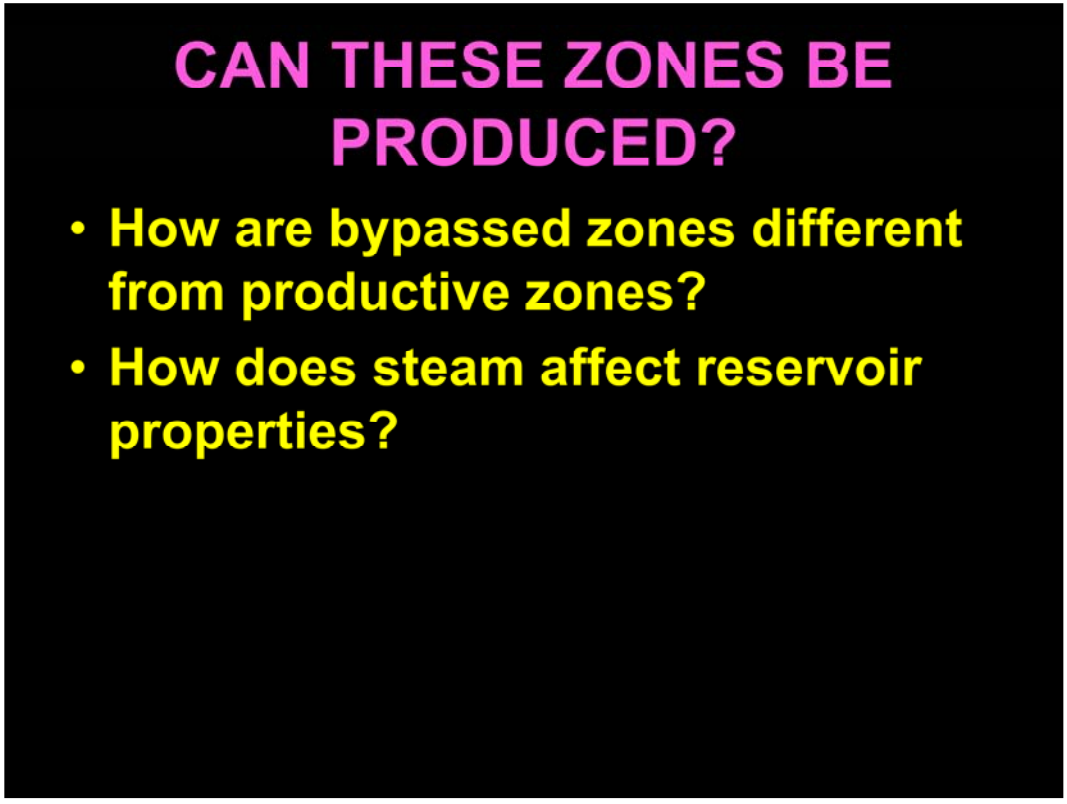

We will now look at the effects of steam injection on these rocks.

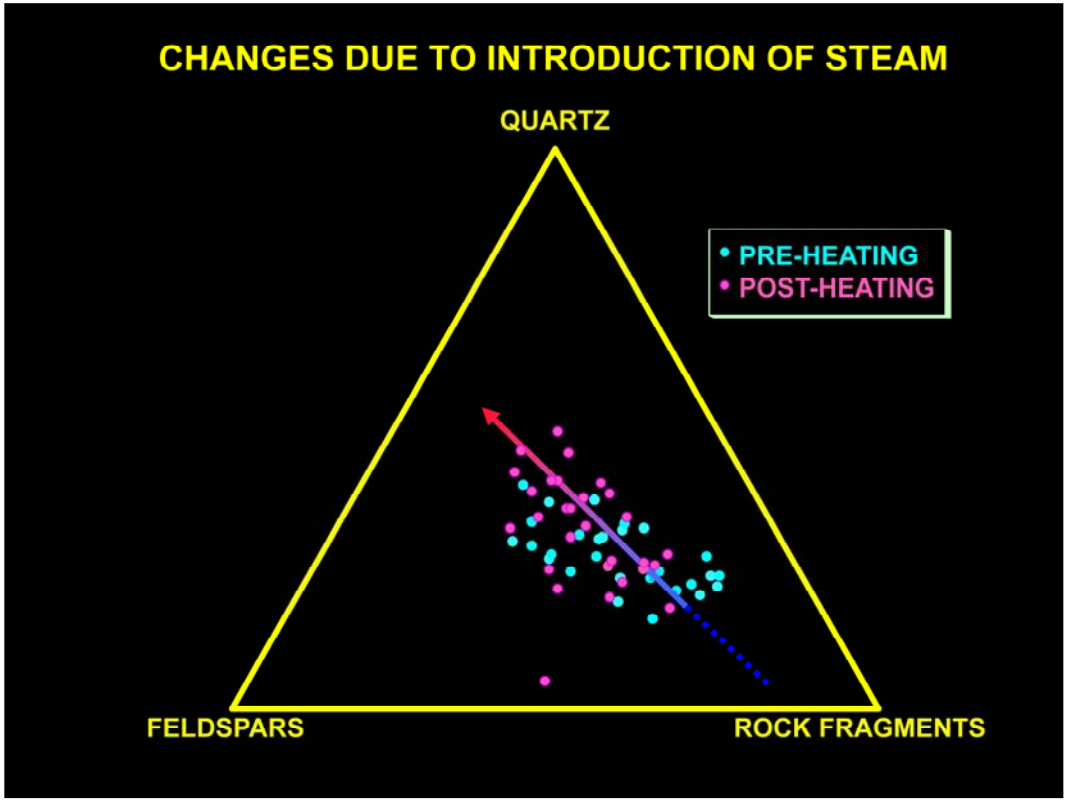

Here is the compositional data for pre-heated sands plotted according to the methodology of Dott (1964) and Pettijohn et al. (1987) that was shown earlier. If post-heating samples are added to the diagram, there is a shift away from the rock fragment corner and also away from the feldspar axis. This shift reflects dissolution of feldspars and disintegration of plutonic rock fragments as the feldspars dissolve.

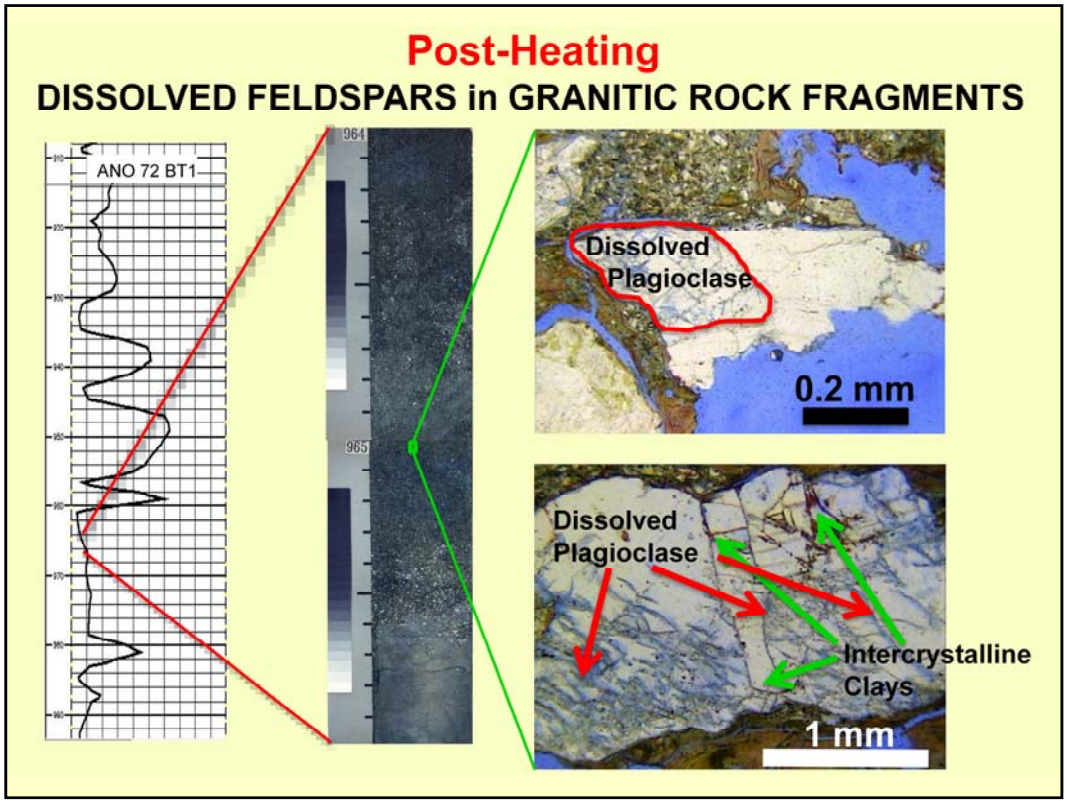

These images from a post-heating sample show granitic microphanerites containing partially dissolved plagioclase crystals. The lower photomicrograph also shows dissolution and subsequent precipitation of clays along intercrystalline boundaries as the rock fragment began to break apart.

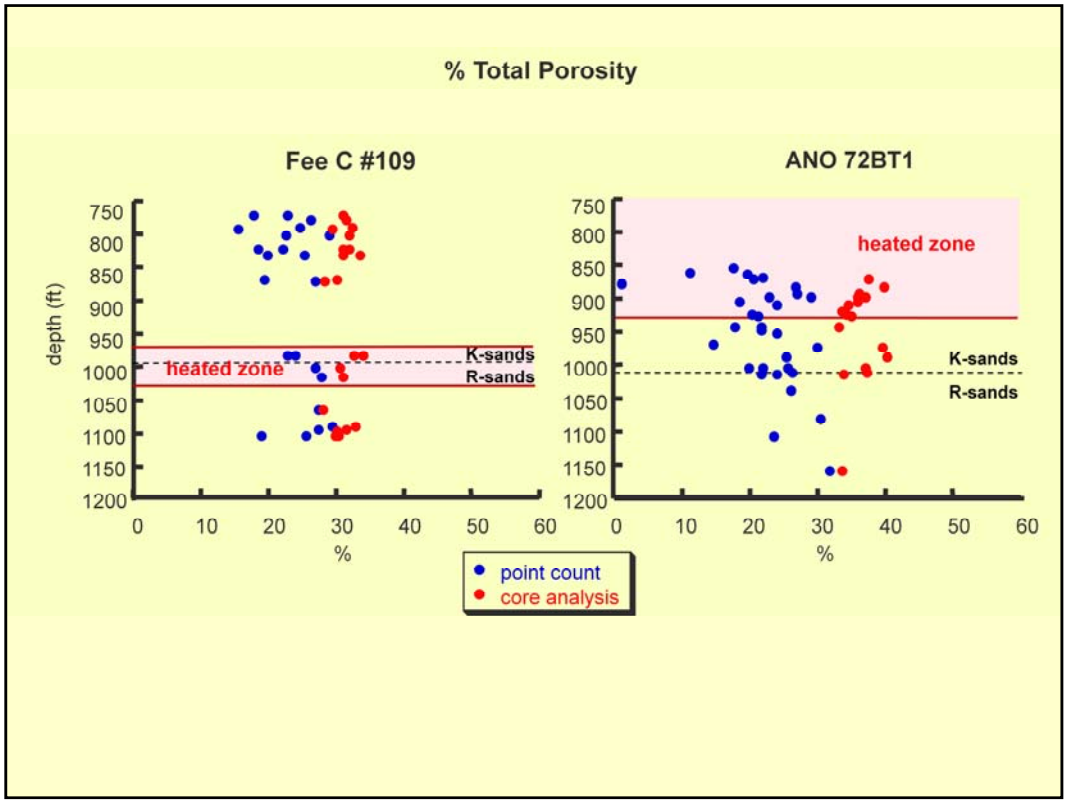

These diagrams show porosity as determined by point-counting petrographic thin sections and by conventional core analysis for two cores, each of which contain heated and unheated zones. There is a small increase in total porosity in the heated samples from the upper (K) sands as determined using conventional core analysis. This would be expected with the dissolution of feldspars. However in the point count data, which includes only those pores large enough to see with a petrographic microscope, no change in porosity is indicated. Thus, any increase in porosity has occurred in microporosity rather than what might be characterized as the effective porosity that can be observed in thin section.

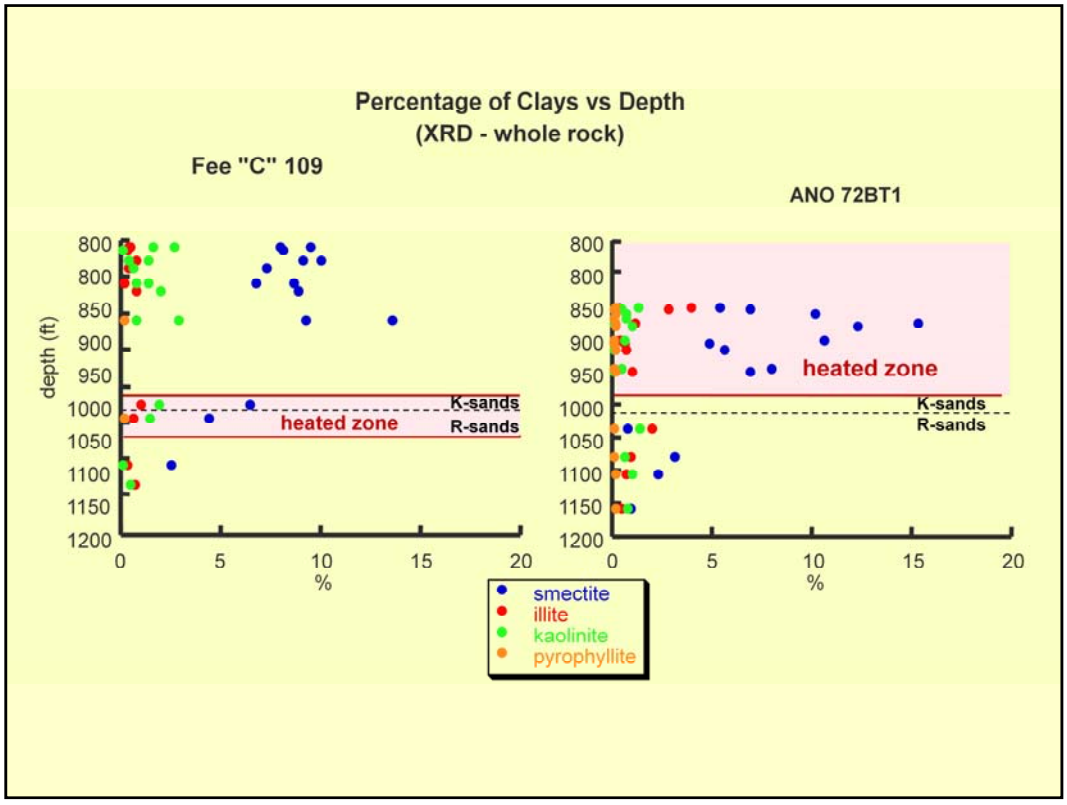

These diagrams show the composition of clay minerals in unheated and heated samples. Illite probably reflects fine-grained micas. Kaolinite is minor and shows a slight reduction due to heating. Smectite shows an increase in both heated zones. These analyses did not characterize smectite type or distinguish smectite from smectite-rich mixed-layer illite/smectite.

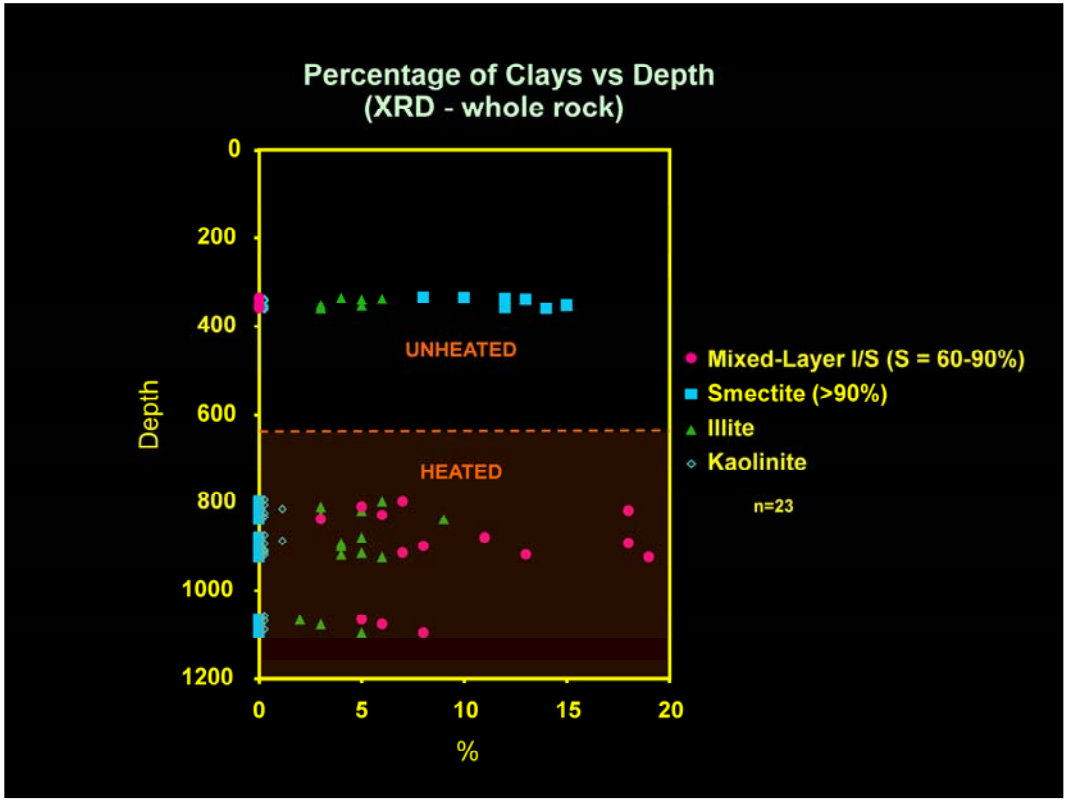

A second suite of samples was collected from decreasing-resistivity zones, some heated and some not heated. These analyses distinguished between smectite and mixed-layer illite/smectite and also characterized the mixed-layer clays. The unheated samples contain relatively pure smectite as might be expected from shallow burial diagenesis in the presence of fresh groundwater. In contrast, the heated samples contain random-ordered mixed-layer illite/smectite containing 60-90% smectite layers.

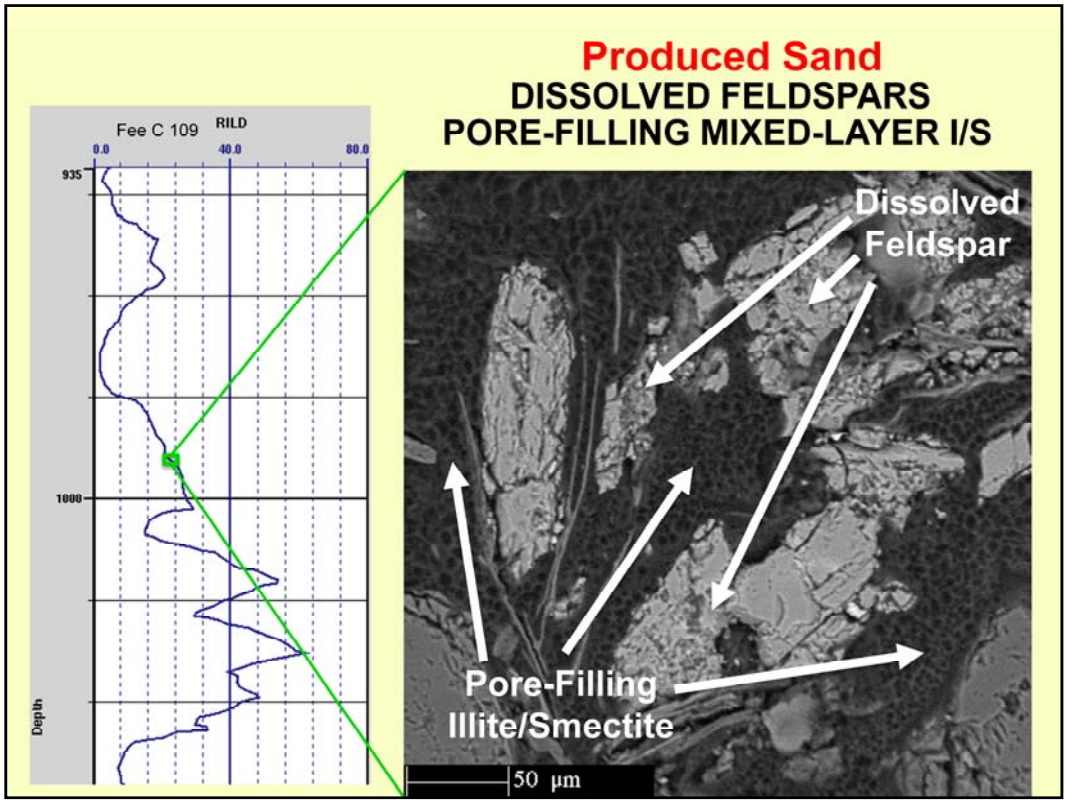

This is a back-scattered-electron image from a heated sand showing a partially dissolved feldspar and mixed-layer illite/smectite filling pores, including those created by feldspar dissolution. There is a significant amount of intercrystalline microporosity within the clay, but the pores are very small.

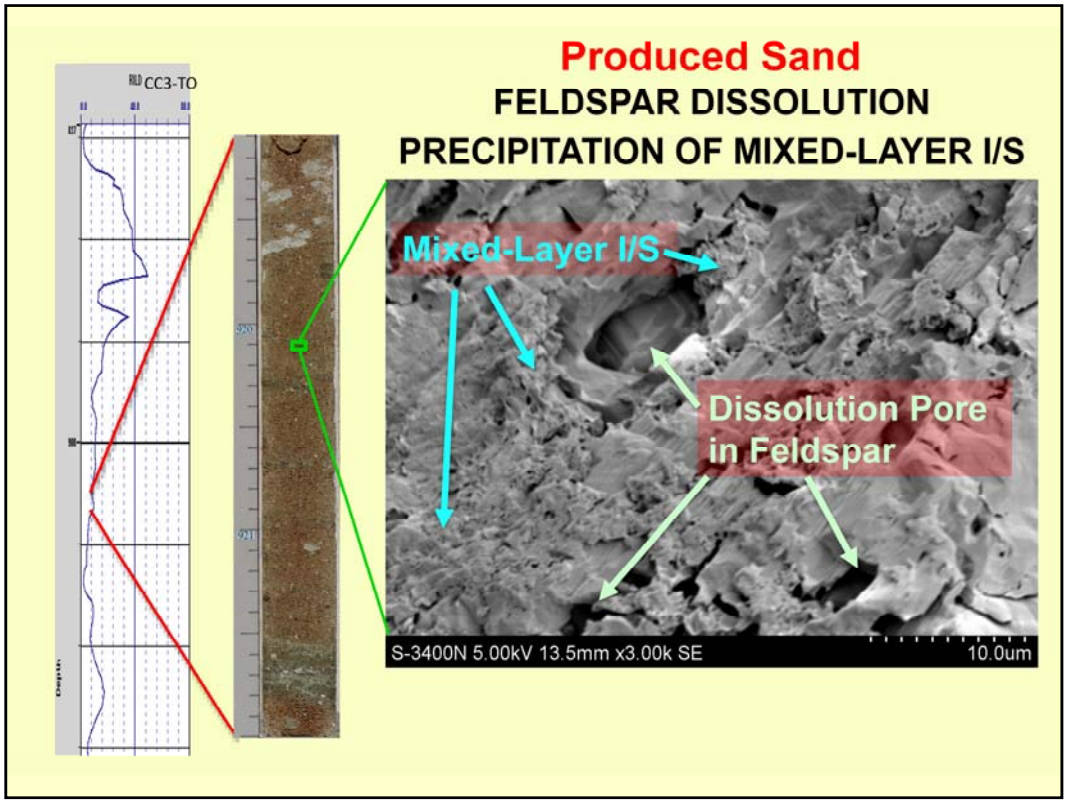

Here is an SEM image of a leached feldspar grain from a produced sand. There is also pore-filling illite/smectite, including some that formed within the dissolution pores in the feldspar.

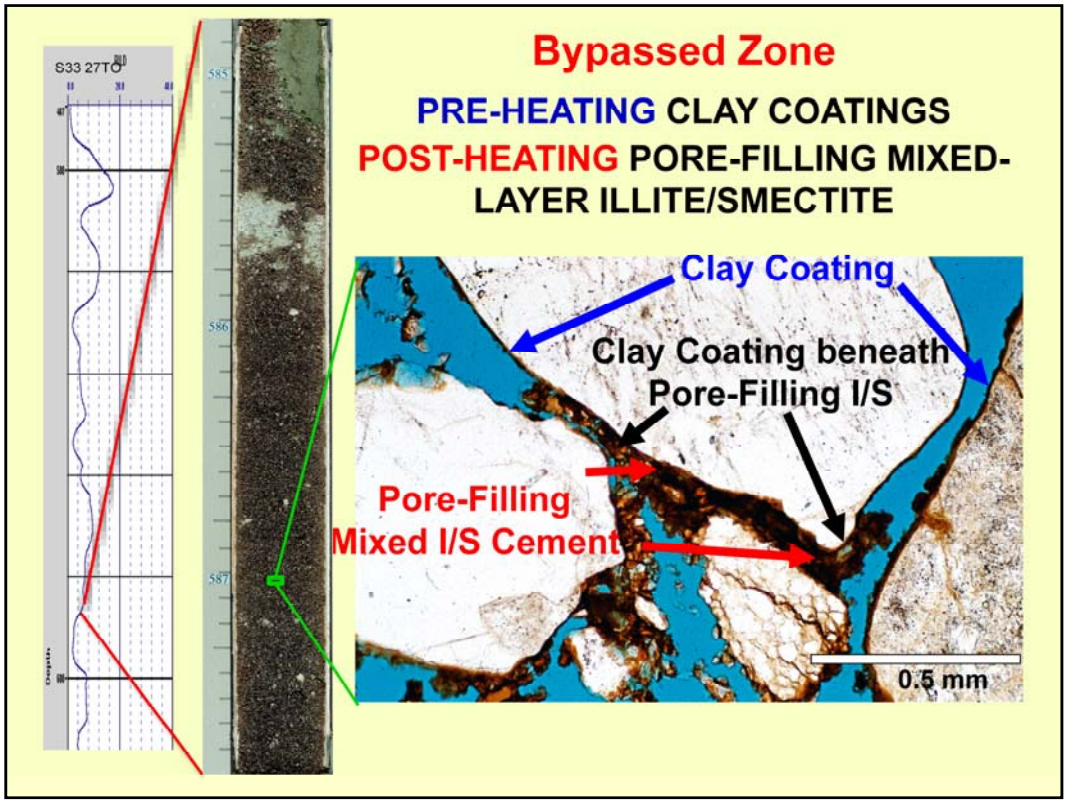

This sample is from a bypassed zone. The grains have clay coatings that most likely formed by normal diagenetic processes prior to heating. There are also mixed-layer clays that have formed on top of the clay coatings. These have filled some pore spaces and formed bridges across other pore spaces.

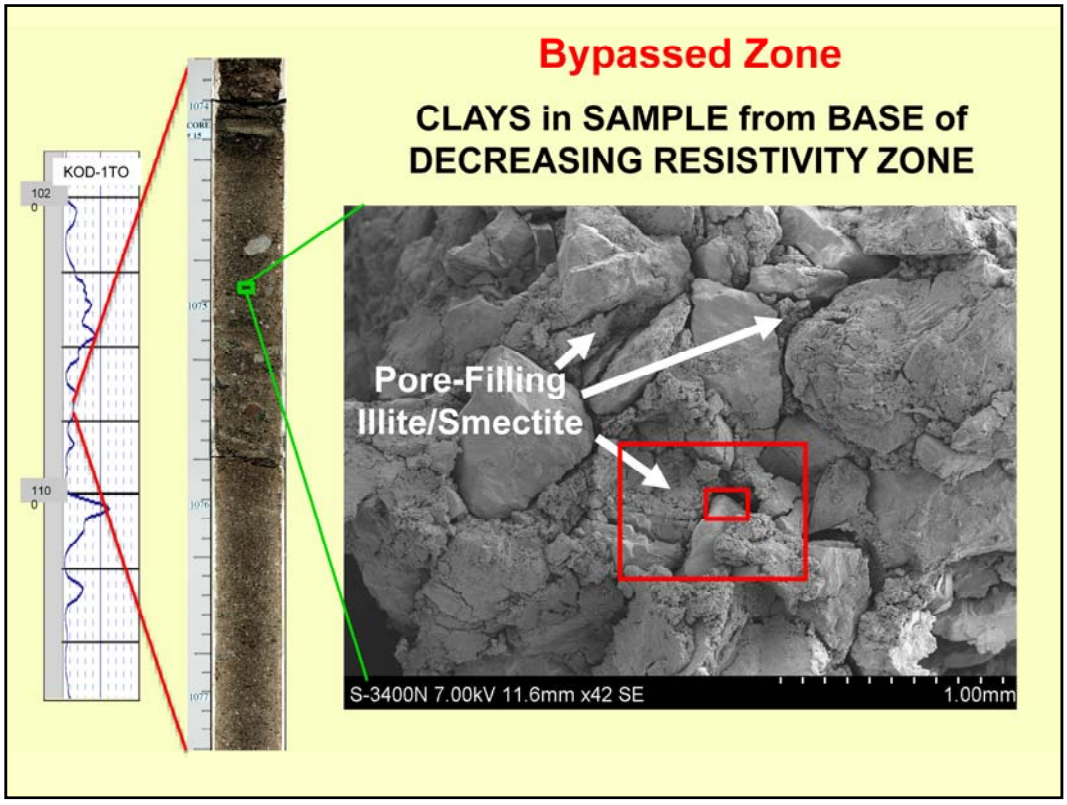

Here is a post-heating sample of sand from one of the bypassed zones. Between the grains there are masses of pore-filling mixed-layer illite/smectite. The large pores along grain edges are artifacts formed during sample preparation and reflect the difficulty in working with these unconsolidated samples. The next slide will zoom in on the area defined by the smaller rectangle and the following slide will zoom out to the area defined by the larger rectangle.

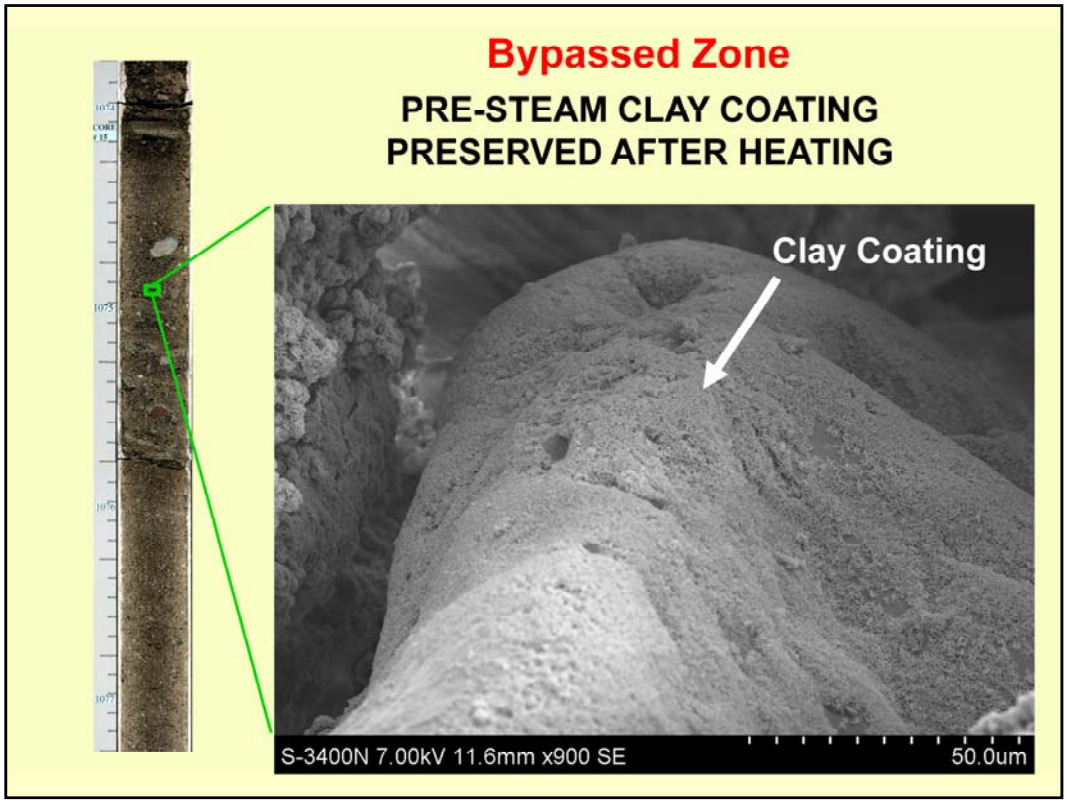

This sand grain is covered by a clay coating that probably formed during diagenesis prior to heating by steam.

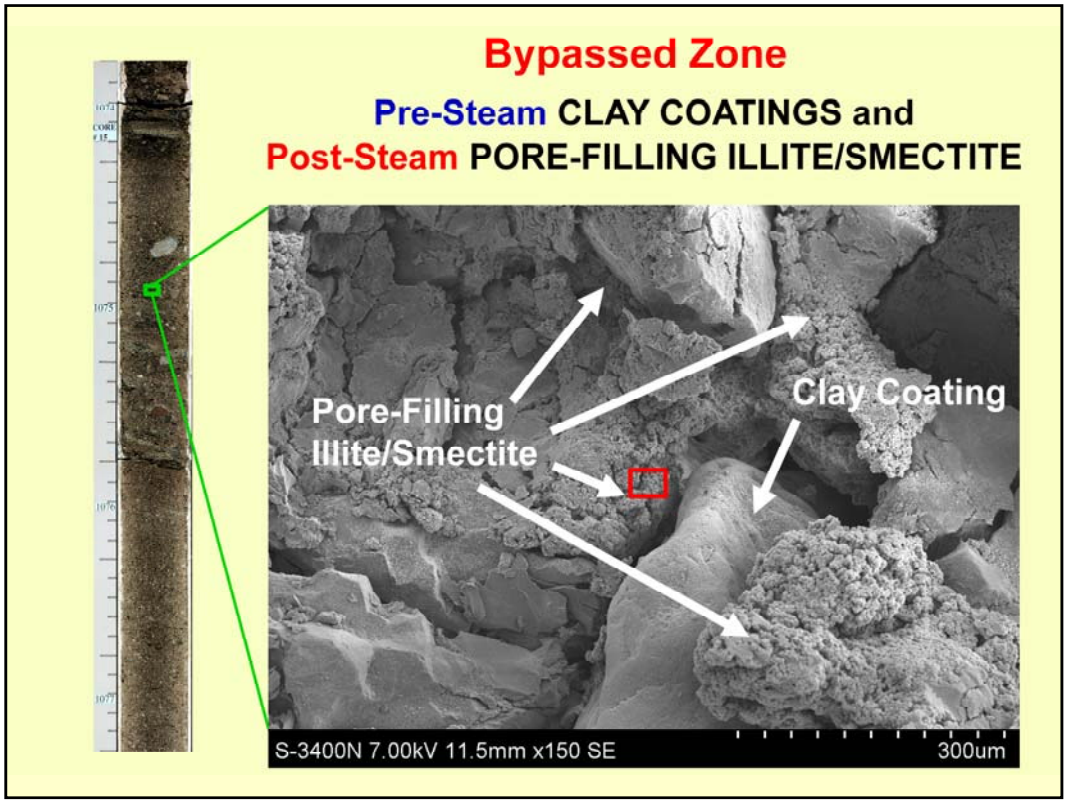

Zooming out, the same sand grain with its pre-heating clay coating is visible in the lower half of the image. The intergranular material in this sample is mostly made up of post-heating pore-filling illite/smectite. The next slide will zoom in on the area defined by the rectangle.

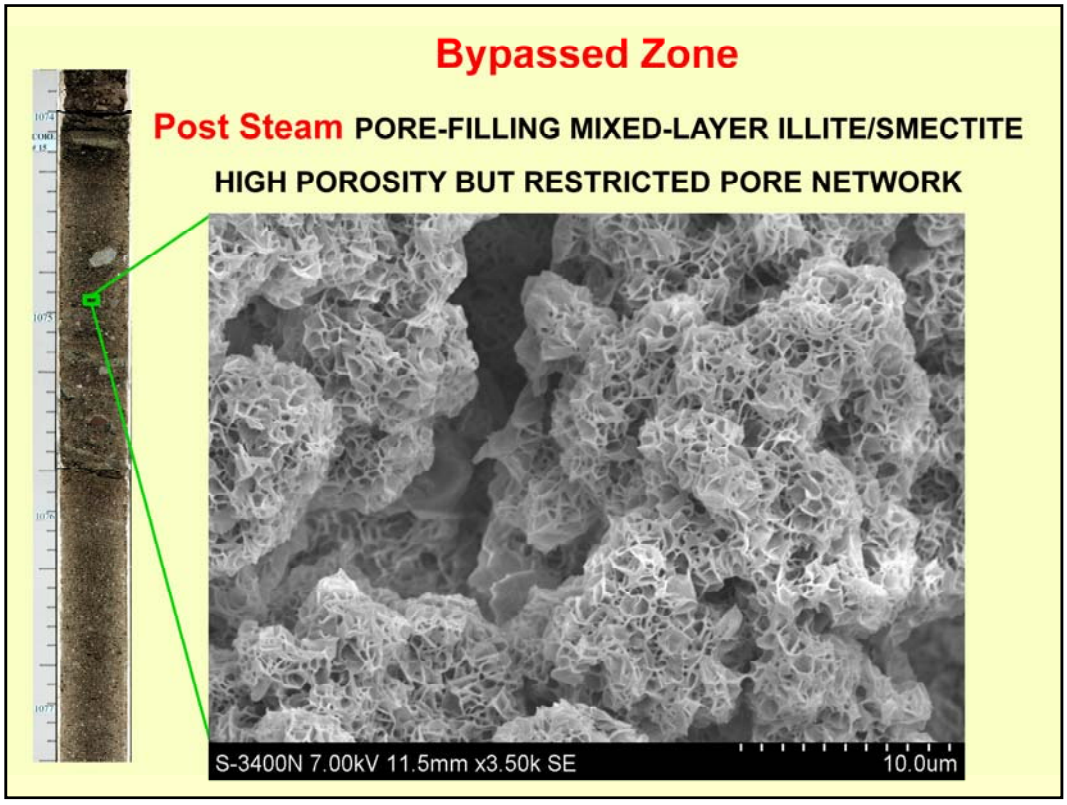

The pore-filling clay consists of intergrown globs (for lack of better term) of finely crystalline mixed-layer illite/smectite. There is a significant amount of intercrystalline microporosity within the clay, but the average pore diameter is on the order of one micron. The large fracture is a sample-preparation artifact.

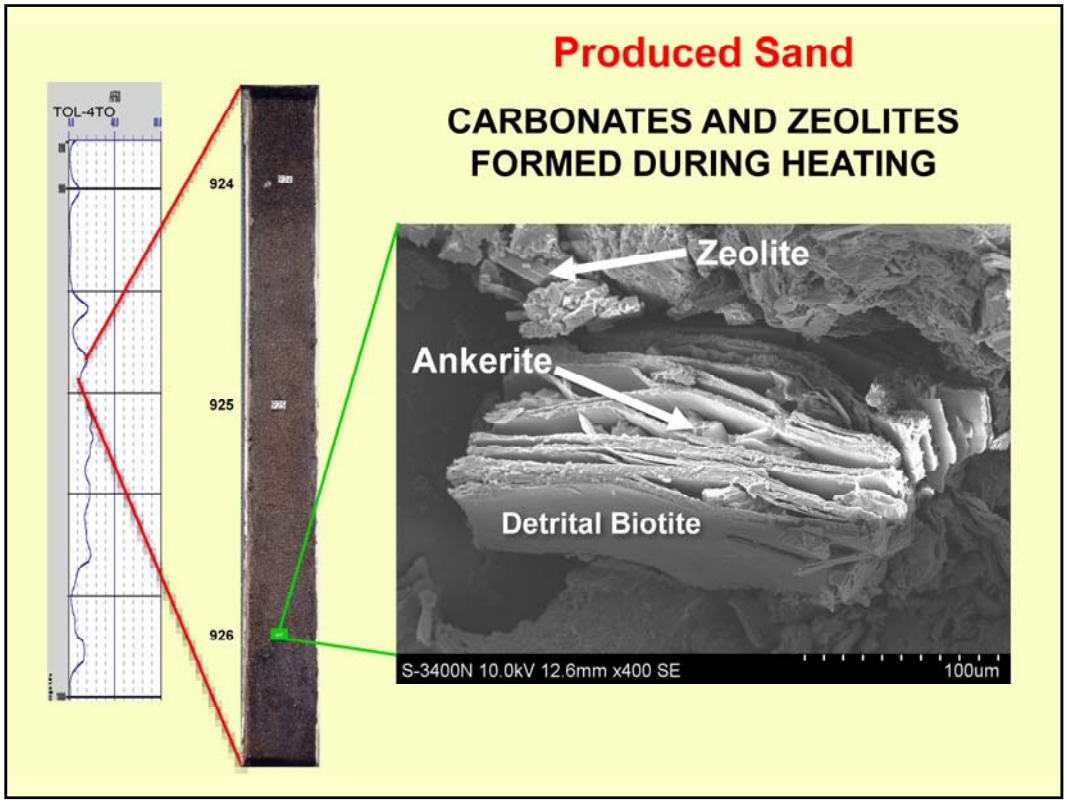

Other minerals formed during heating that may have affected porosity and permeability include carbonates and zeolites. In this example ankerite formed along cleavage surfaces in biotite thus expanding the biotite into the surrounding pore space. Clinoptiololite-heulandite crystals formed contemporaneously with, and are intergrown within, the pore-filling illite/smectite.

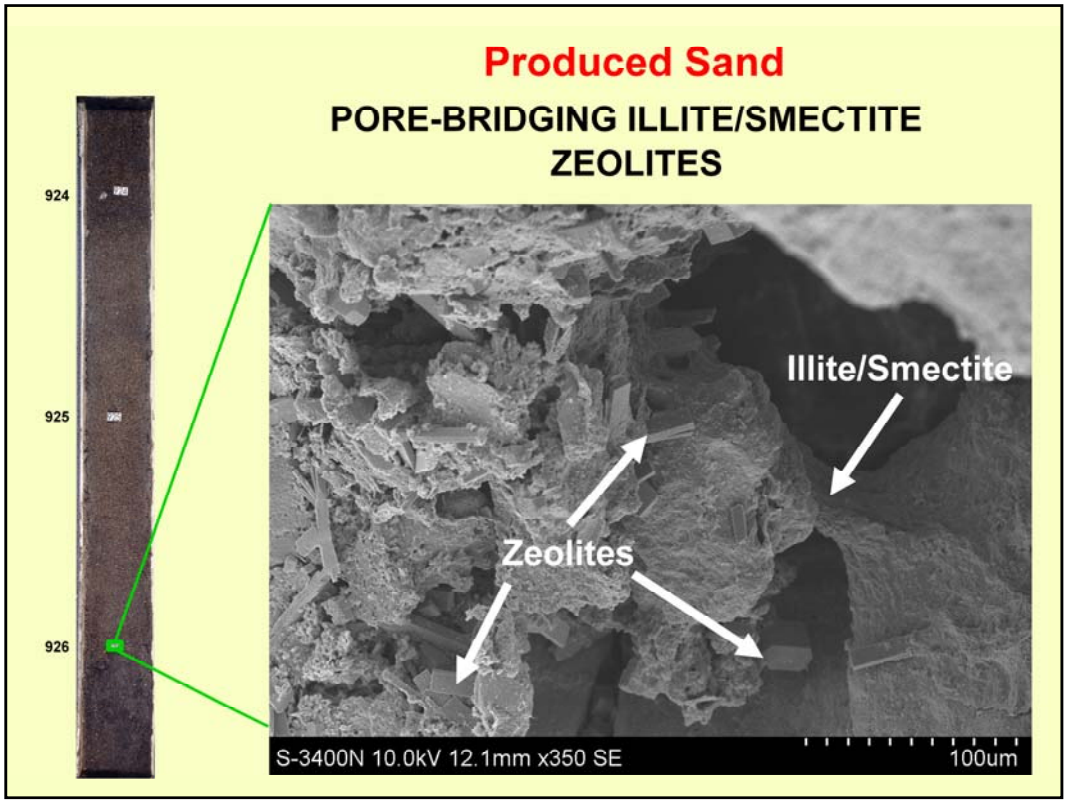

This SEM image, from a produced sand, shows another example of pore-bridging illite/smectite intergrown with clinoptilolite-heulandite crystals.

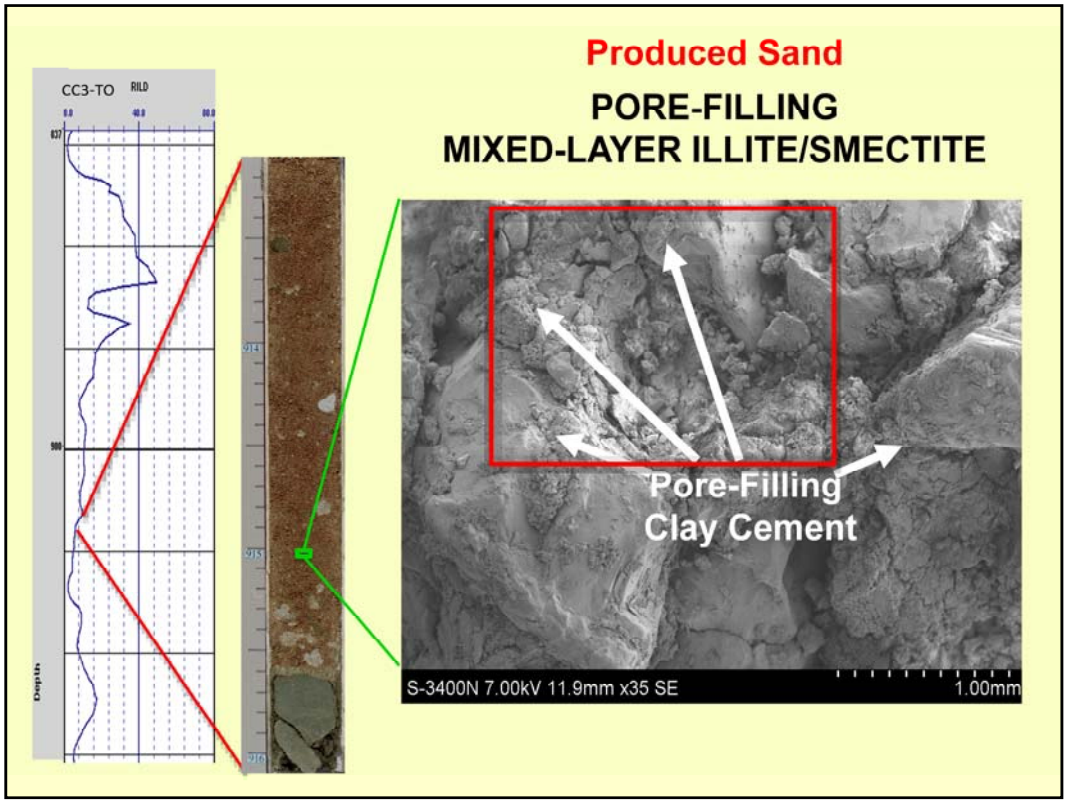

This SEM image, from a produced sand, shows mixed-layer illite/smectite that mostly filled intergranular porosity after removal of oil. The next slide will zoom in on the area defined by the rectangle.

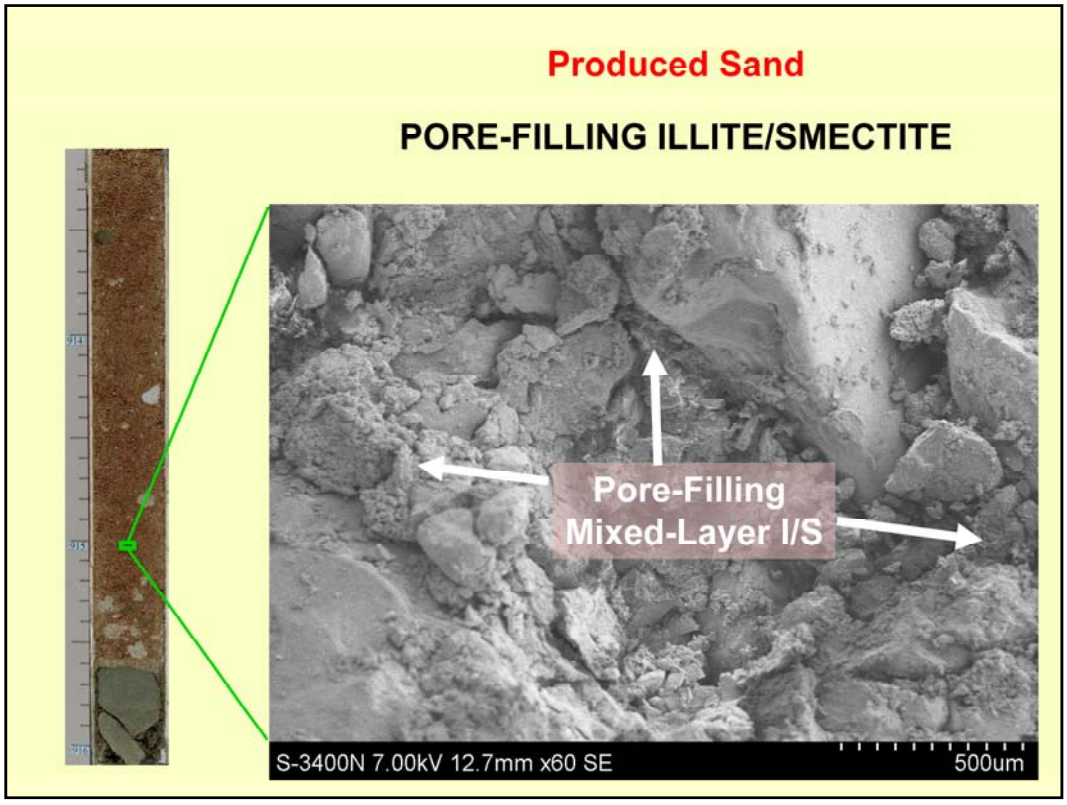

This image shows the nature of the pore-filling illite/smectite, including the same globular texture that was observed in post-heating samples from the bypassed zones.

CONCLUSIONS

- Bypassed oil resides in sediments with gradually decreasing resistivity curves at their bases
- The decreasing resistivity curves reflect a change from moderately sorted sands to poorly sorted gravels with less open pore networks

CONCLUSIONS

- Heating during steam injection resulted in dissolution of feldspars, decomposition of rock fragments, changes in clay compositions, and precipitation of pore-filling mixed-layer illite/smectite

- Precipitation of mixed-layer illite/smectite may have reduced permeability thereby resulting in diminished production

CONCLUSIONS

- This shows the usefulness of obtaining cores and studying the rocks to augment well logs and other geophysical or petrophysical data when characterizing a reservoir and planning an EOR program

REFERENCES:

Dickinson, W.R., 1970, Interpreting detrital modes of graywacke and arkose: Journal of Sedimentary Petrology, v. 40, p. 695-707.

Dott, R.H., 1964, Wacke, graywacke, and matrix — what approach to immature sandstone classification?: Journal of Sedimentary Petrology, v. 34, p. 625-632.

Kodl, E.J., 1988, Texaco, unpublished in-house report.

Pettijohn, F. J., Potter, P. E., and Siever, R., 1987, Sand and Sandstone (2nd): New York, Springer-Verlag, 553 p.